

CHAPTER TWO

Preparation & Characterization of

Ru²⁺- and Re⁺-modified Pseudomonas aeruginosa Azurins

2.1 ABSTRACT

Three new high-potential ruthenium complexes for protein modification have been synthesized and characterized. $[\text{Ru}(\text{trpy})(\text{tfmbpy})]^{2+}$ has optimal redox and photophysical properties for protein electron transfer experiments. Proteins with a 3-nitrotyrosine moiety were successfully made and characterized for the investigations of hopping through nitrotyrosine. Protocols for the expression, labeling, and purification of modified proteins were developed and shown to be quite general. All together, eleven modified proteins were prepared and characterized.

2.2 INTRODUCTION

Design of Hopping Systems

The simplest hopping center has three redox centers: the photosensitizer, one intermediate aromatic amino acid, and the metal that is resident to the protein. Two "hops" accomplish the transfer of an electron between the two metal centers. **Figure 2.1** depicts two different hopping systems, with the hops in each system depicted with a blue arrow.

There are a few considerations to keep in mind when engineering a hopping system. For instance, in the systems described in **Figure 2.1**, 1) the system will be installed on a protein, so the protein must be easy to manipulate and fairly stable; 2) the

protein to be utilized ought to have a reduction potential that is fairly low, so that hopping is favorable; 3) the reduction potential of the intermediate must be low enough to be oxidized by the metal label, but high enough to drive the subsequent oxidation of the metal resident to the protein; and 4) the reduction potential of the metal label's excited state, or its oxidized state must be high enough to drive the entire process.

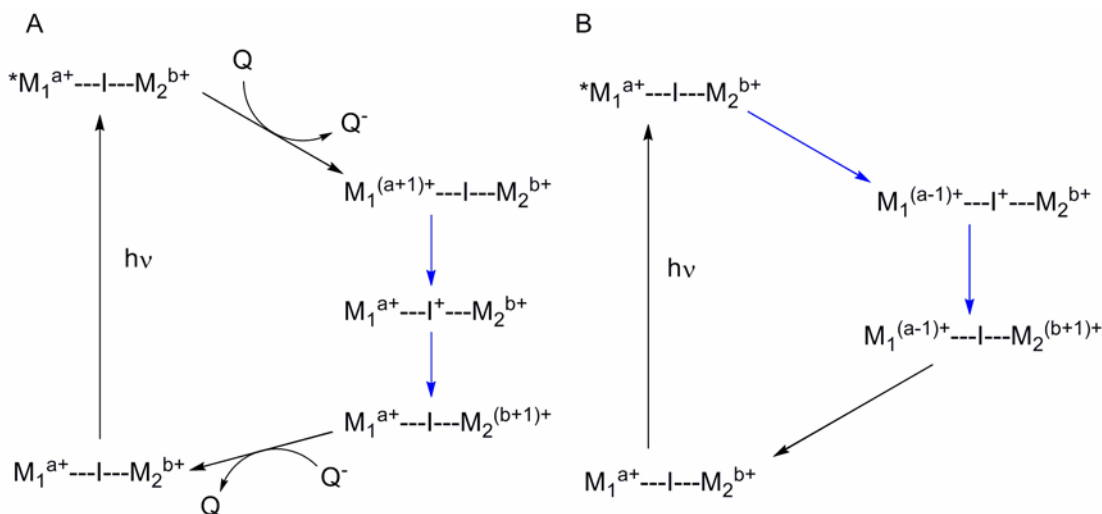


Figure 2.1. Two different hopping systems. In both cases, the two hops are highlighted in blue. **A.** The photosensitizer M_1 is excited then oxidized by an external quencher Q . Intermediate I reduces the oxidized M_1 , and is then reduced by M_2 . The oxidized M_2 is eventually reduced by the reduced Q and the system returns to ground state. **B.** The photosensitizer M_1 is excited and then reduced by the intermediate I . Oxidized I is reduced by M_2 , then single-step charge recombination occurs to regenerate the ground state system.

Pseudomonas aeruginosa azurin

The cupredoxin azurin from *Pseudomonas aeruginosa* is an ideal protein on which to execute hopping studies. Azurin is a small, 128 residue protein that shuttles electrons between cytochrome 551 and nitrite reductase in the denitrifying chains in bacteria.^{1,2} The cupredoxins are known for their intense blue color, which originates in the unique binding motif of the copper center.³⁻⁶ The copper is held in a trigonal bipyramidal geometry; His46, His117, and Cys112 bind the metal in the equatorial plane,

and the sulfur of Met121 and the carbonyl oxygen of Gly45 ligate axially (**Figure 2.2**). The ligand-to-metal charge transfer from the Cys112 into the copper gives azurins (and for that matter, all type I copper proteins) their color. The reduction of the copper is measured to be approximately 0.31 V *v.* NHE.⁷

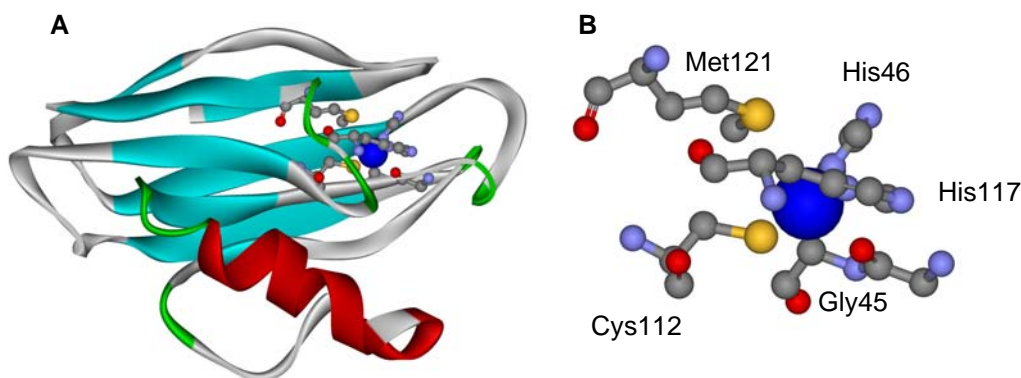


Figure 2.2. Crystal structure of *Pseudomonas aeruginosa* azurin (PDB code 1AZU). **A.** Total structure, 128 amino acids, β -barrel structure comprising eight anti-parallel β strands. **B.** The ligands of the copper in *P. aeruginosa* azurin; trigonal bipyramidal coordination: His46, H117, Cys112 ligate the metal on the equatorial plane. The sulfur of Met121 and the carbonyl oxygen of Gly45 coordinate axially.

Protocols were developed to express *Pseudomonas aeruginosa* azurin and the structure appeared to be quite robust to mutations.⁸ Because the protein has an appropriate potential, and is easy to work with, it has been utilized before in the metal-modified metalloprotein program. Electronic coupling of β -sheet structures was studied utilizing azurin's β -barrel structure.^{9,10} The kinetics of electron transfer were fairly well-behaved, plotting out almost linearly on a distance *v.* log rate plot, the distance-decay β value being calculated to be approximately 1.00 \AA^{-1} .

Furthermore, electron transfer studies done on single crystals of azurin revealed the electron transfer kinetics were the same in azurin, regardless of whether or not the protein was in a crystal or in solution.¹¹ This substantiated the studies done before, as it was

now clear that the structures in the solution studies were similar to the natural structure of the system. The report also included crystal structures of the reduced forms of azurin, which illustrated that upon the metal's reduction, the ligands did not reorient themselves, making inner-sphere reorganization energy quite small; the coordination environment is constrained by a "cage" of hydrogen bonds, in a cluster of hydrophobic residues.

Given the plethora of established protocols for expressing and labeling azurin mutants, its well-behaved kinetics, as well as appropriate reduction potential, it is clearly one of the most attractive proteins on which to build hopping systems. Only a few adjustments have to be made to make the system appropriate: the wild-type surface H83 will be mutated to prevent mislabeling when targeting the other sites, and the resident tyrosines (Tyr72 and Tyr108) and tryptophan (Trp48) will be mutated so that any rate enhancement exhibited (or radicals observed) will be derived from the system of interest. All hopping systems are constructed on the All-Phe azurin mutant: W48F/Y72F/H83Q/Y108F, and will be hereafter abbreviated simply as Az.

Previously labeled sites of the appropriate distance ($\sim 20\text{--}25$ Å) for hopping studies include the wild-type surface His83 and sites 107, 124, and 126, so they are the first choices for metal modification. The hopping residue will be installed along the established tunneling pathways from these sites to the copper.

Reduction Potentials & Photosensitizers

When investigating hopping, the reduction potentials of all redox centers involved must be considered (**Table 2.1**). The reduction potential of one metal center is fixed: the $\text{Cu}^{2+/+}$ couple of azurin is measured to have a reduction potential of 0.31 V v. NHE.⁷

| redox couple | E° (V v. NHE) | reference |
|--|---------------|-----------|
| Cu ^{2+/+} | 0.31 | a |
| Ru(bpy) ₂ (im)(HisX) ^{3+/2+} | 1.08 | b |
| Re(phen)(CO) ₃ (HisX) ^{2+/+} | 2.0 | c |
| TrpH ^{•+} /TrpH | 1.15 | d |
| Trp [•] /TrpH | 1.01 | d |
| Trp [•] /Trp ⁻ | 0.41 | e |
| TyrH ^{•+} /TyrH | 1.45 | f |
| Tyr [•] /TyrH | 0.91 | d,g,h |
| Tyr [•] /Tyr ⁻ | 0.72 | d,g,h |
| NO ₂ Tyr [•] /NO ₂ Tyr ⁻ | 1.07 | i |

Table 2.1. Estimated reduction potentials for redox couples relevant to multistep electron tunneling studies. ^aPascher, T.; Karlsson, B.G.; Nordling, M.; Malmstrom, B.G.; Vanngard, T. *Eur. J. Biochem.* **1993**, *212*, 289–296. ^bDi Bilio, A.J.; Hill, M.G.; Bonander, N.; Karlsson, B.G.; Villahermosa, R.M.; Malmstrom, B.G.; Winkler, J.R.; Gray, H.B. *J. Am. Chem. Soc.* **1997**, *119*, 9921–9922. ^cConnick, W.B.; Di Bilio, A.J.; Hill, M.G.; Winkler, J.R.; Gray, H.B. *Inorg. Chim. Acta* **1995**, *240*, 169–173. ^dHarriman, A. *J. Phys. Chem.*, **1987**, *91*, 6102–6104. ^ecalculated, given potential in ref.d and pK data from Remers, W.A. in *Indoles: Part One*; Houlihan, W.J., Ed.; Wiley-Interscience: New York, 1972, Vol. 25, 1-226. ^fcalculated, given the potential in refs. d,g,h, and pKs mentioned therein. ^gSjödin, M.; Styring, S.; Åkermark, B.; Sun, L.; Hammarström, L. *J. Am. Chem. Soc.*, **2000**, *122*, 3932–3936. ^hMagnuson, A.; Frapart, Y.; Abrahamsson, M.; Horner, O.; Åkermark, B.; Sun, L.; Girerd, J.J.; Hammarström, L. *J. Am. Chem. Soc.* **1999**, *121*, 89–96. ⁱLeigh, B.S. (*unpublished results*).

Previous attempts by former Gray group graduate students Drs. William A. Wehbi¹² and Jeremiah E. Miller¹³ to engineer systems to exhibit hopping kinetics through tyrosine and tryptophan were thwarted by one very frustrating complication; once oxidized, the radical cation is easily deprotonated and the reduction potential of the resulting neutral radical is not high enough to drive the subsequent tunneling reaction (**Figure 2.3**).



Figure 2.3. Reduction potentials and pK_as of relevant oxidation/protonation states of tryptophan and tyrosine¹⁴⁻¹⁷

In order to avoid problems of deprotonation, it is proposed to study hopping through the tyrosine analog 3-nitrotyrosine. The pK_a of the proton is measured to be around 7; if the hopping experiments on the system are executed at a pH above 7 the residue will already be deprotonated, so there will only be one reduction potential to worry about. The relevant reduction potential is measured to be 1.07 V *v.* NHE,¹⁸ which is well within range of those of tyrosine and tryptophan, so the residue will likely participate in hopping. Finally, installation of the nitro group onto tyrosine is easily achieved utilizing protocols established in the late 1960s.¹⁹⁻²³ A tyrosine will be introduced to the site of interest using site-directed mutagenesis, and the protein will be exposed to tetranitromethane to achieve the substitution.

In the choice of metal label, a high-potential photosensitizer will have to be utilized; if either of the strategies in **Figure 2.1** are to work, the reduction potential of either the excited (*M₁^{a+}) or oxidized (M₁^{(a+1)+}) states must be high enough to drive the overall electron transfer. Wehbi and Miller's first attempts were carried out with the rhenium compounds, Re(phen)(CO)₃⁺ and Re(dmp)(CO)₃⁺ (dmp = 4,7-Dimethyl-1,10-phenanthroline). Both the *Re⁺ and Re²⁺ states have high reduction potentials (**Figure 2.4**).

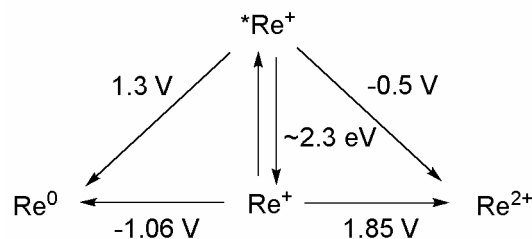


Figure 2.4. Modified Latimer diagram of $\text{Re}(\text{phen})(\text{CO})_3^{+24}$. Constructed from values obtained in acetonitrile, using a Ag/AgCl reference electrode.

Rhenium, while being of the appropriate reduction potential, is optically inactive in both Re^+ and Re^{2+} states, which limits the information that can be obtained on the metal's oxidation state. The Gray group has had considerable experience working with ruthenium photosensitizers in the metal-modified metalloprotein program,^{9,10,25-28} so it is natural to once more consider this oft-used option. The reduction potential of $\text{Ru}(\text{bpy})_2(\text{im})(\text{HisX})^{3+/2+}$ is 1.08 V *v.* NHE, so it is still a bit too low for the proposed studies. However, the potential of the metal can be tuned through substitution onto the bipyridine ligand framework. This approach has been utilized before in the investigation of the effect of driving force on electron transfer kinetics.²⁶ The highest potential accessed in these studies was 1.26 V *v.* NHE, which was achieved by installing amides in the 4,4' positions. It is hoped that by substituting with an even more electron-deficient group, such as trifluoromethyl, the potential can be raised even more. For this reason, labels utilizing bis-trifluoromethyl-substituted bipyridine (tfmbpy) ligands will be pursued for this newest generation of hopping systems.

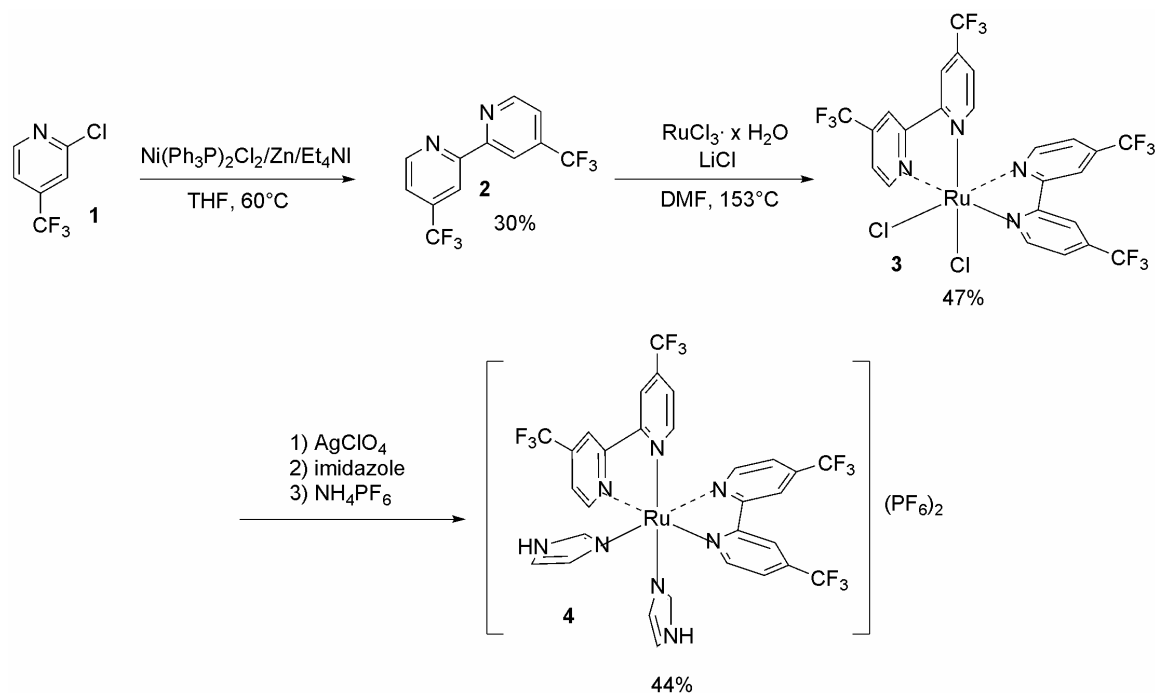
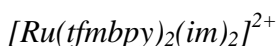
Chapter Outline

This chapter provides the protocols used in the synthesis of all the metal-modified metalloprotein systems studied in this dissertation. First, the synthesis and

characterization of metal labels are addressed; more than one ruthenium label was synthesized, but one was clearly easier to work with, and had appropriate photophysical and electrochemical properties. Secondly, the preparation of protein, including the preparation of the 3-nitrotyrosine-substituted mutants is outlined. Through the course of studying the nitration reaction, unfolding studies were made, the results of which are also included. Thirdly, protocols to install the label onto the protein surface are listed. The experimental section includes extensive details on the synthesis of these systems, as well as on how samples were prepared for laser spectroscopy measurements.

2.3 RESULTS AND DISCUSSION

Metal Labels



Scheme 2.1. Synthesis of $[Ru(tfmbpy)_2(im)_2](PF_6)_2$

$[\text{Ru}(\text{tfmbpy})_2(\text{im})_2]^{2+}$ was synthesized as described in **Scheme 2.1**; only a few modifications had to be made to the established protocol to achieve synthesis of the compound. The nickel-catalyzed coupling reaction of the monomer (**1**) afforded tfmbpy (**2**) in low yields. The ligand was installed onto the ruthenium to generate $\text{Ru}(\text{tfmbpy})_2\text{Cl}_2$ (**3**) in moderate yield. Due to the unreactive nature of the $\text{Ru}(\text{tfmbpy})_2\text{Cl}_2$ compound, many different methods were attempted to generate the imidazole-ligated product (**4**). It was found that removal of the chlorines with silver to generate an acetone-ligated intermediate was essential. Subsequent addition of the imidazole generated the product.

The absorbance and fluorescence spectra of $[\text{Ru}(\text{tfmbpy})_2(\text{im})_2](\text{PF}_6)_2$ in acetone are shown in **Figure 2.5**. The metal-to-ligand charge transfer from the t_{2g} to π^* of the tfmbpy ligand is observed at 514 nm and excitation at this wavelength results in emission that maximizes at 707 nm in water. The lifetime of the excited state was found to be 33 ns in water (**Figure 2.6**). This lifetime is much shorter than is desired; traditionally, ruthenium labels for electron transfer studies have had lifetimes of at least 100 ns.^{9,10,25-28} However, it has been observed that lifetimes of excited states are generally longer in organic solvents and on protein than they are in aqueous environments. This supposition was confirmed: the lifetime was extended to 42 ns in acetone, and 51 ns in acetonitrile. While the lifetime of the excited state is still quite short, it is suspected that it may extend further still when the label is attached onto the protein.

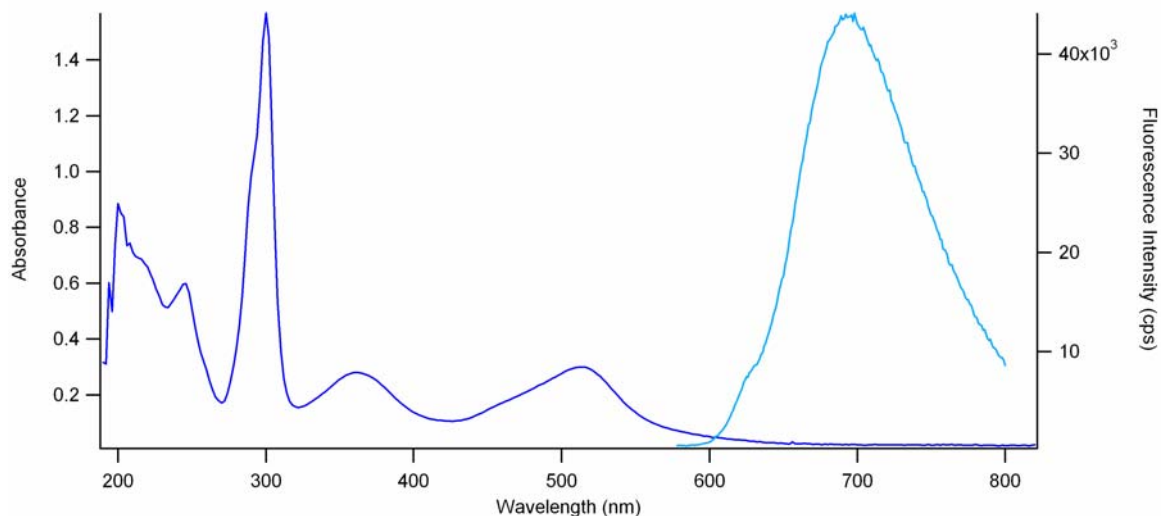


Figure 2.5. Absorption (dark blue) and emission (light blue) spectra of $[\text{Ru}(\text{tfmbpy})_2(\text{im})_2](\text{PF}_6)_2$ in acetone

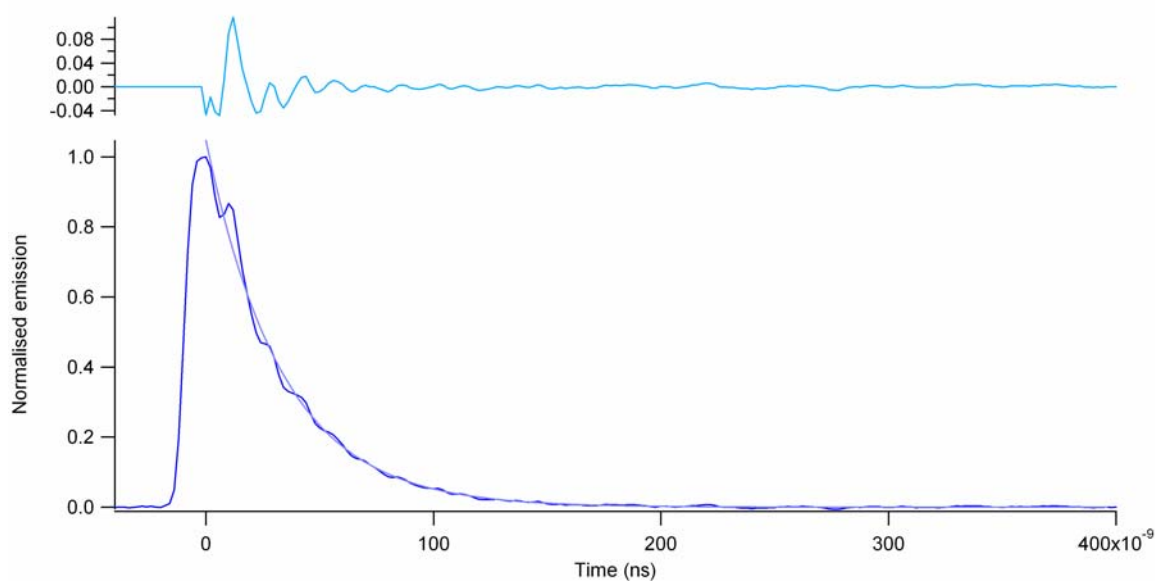
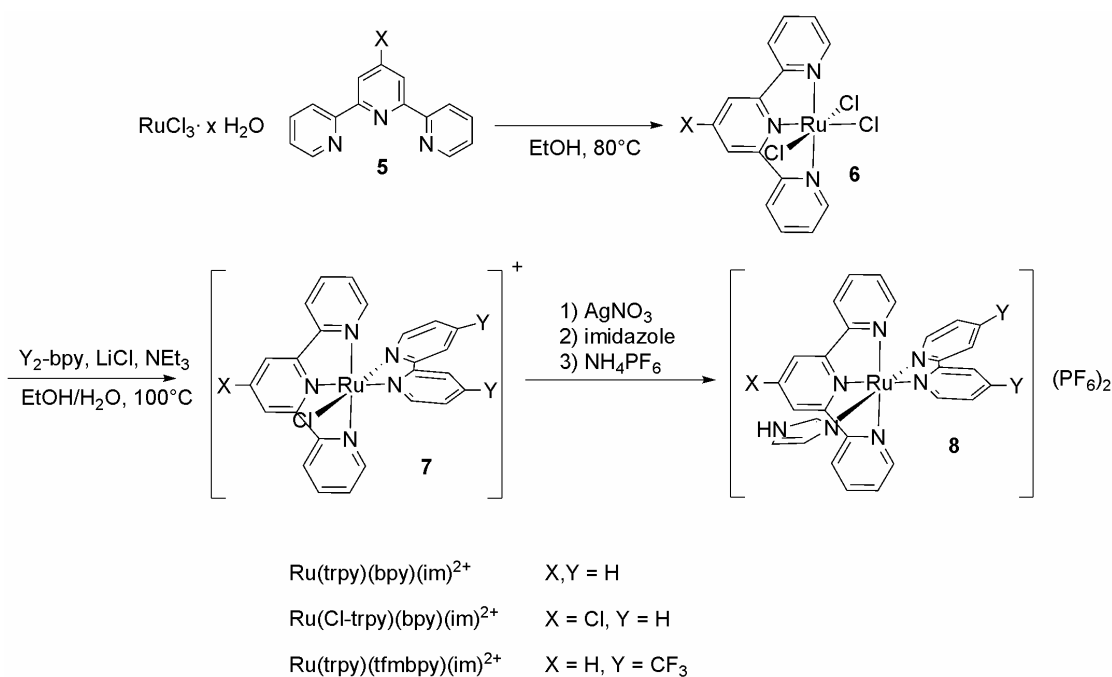


Figure 2.6. Time-resolved emission of $^*[\text{Ru}(\text{tfmbpy})_2(\text{im})_2](\text{PF}_6)_2$ in water. $\lambda_{\text{ex}} = 514 \text{ nm}$, $\lambda_{\text{em}} = 707 \text{ nm}$. Fit to single exponential function, $\tau = 33 \text{ ns}$

The 3-2-1 Architecture

The Gray group has previously worked with the tridentate-bidentate-monodentate architecture (referred hereafter as 3-2-1) on ruthenium: $[\text{Ru}(\text{trpy})(\text{bpy})]^{2+}$ was installed on plastocyanin (trpy = 2,2';6'2"-terpyridine, bpy = 2,2'-bipyridine).²⁸ The measured

reduction potential of $[\text{Ru}(\text{trpy})(\text{bpy})(\text{im})]^{3+/2+}$ was found to be 1.09 V *v.* NHE. So a similar approach to raising the metal's reduction potential by utilizing electron-deficient ligands was to be utilized here. The $[\text{Ru}(\text{Cl-trpy})(\text{bpy})(\text{im})]^{2+}$ and $[\text{Ru}(\text{trpy})(\text{tfmbpy})(\text{im})]^{2+}$ compounds were targeted because Cl-trpy was found to be commercially available and the tfmbpy had already been made for the previous study. In addition, the $[\text{Ru}(\text{trpy})(\text{bpy})(\text{im})]^{2+}$ compound was synthesized for easy comparison of spectroscopic and electrochemical properties.



Scheme 2.2. Synthesis of 3-2-1 ruthenium compounds

Synthesis of these complexes proved to be quite facile (**Scheme 2.2**). Protocols had been established in the literature and were followed with minor modifications. The trpy ligand (**5**) was easily attached to the ruthenium to generate the $\text{Ru}(\text{trpy})\text{Cl}_3$ species (**6**). The ruthenium was reduced and attached to a bidentate ligand in the following slower step to generate the $\text{Ru}(\text{trpy})(\text{bpy})\text{Cl}$ cation (**7**). Because of the previous success

using silver in the $\text{Ru}(\text{tfmbpy})_2(\text{im})_2$ reaction, the same method was tried, and the model compound (**8**) was obtained. The method proved to be robust to changes in reactant structure. Using more electron-withdrawing ligands slowed reactions down and yielded less compound (**Table 2.2**).

| molecule | time | overall yield |
|---|---------|---------------|
| $\text{Ru}(\text{trpy})(\text{bpy})(\text{im})^{2+}$ | 5 days | 43% |
| $\text{Ru}(\text{Cl-trpy})(\text{bpy})(\text{im})^{2+}$ | 8 days | 25% |
| $\text{Ru}(\text{trpy})(\text{tfmbpy})(\text{im})^{2+}$ | 15 days | 14% |

Table 2.2. Overall yields and overall time taken to synthesize three 3-2-1 architecture ruthenium compounds

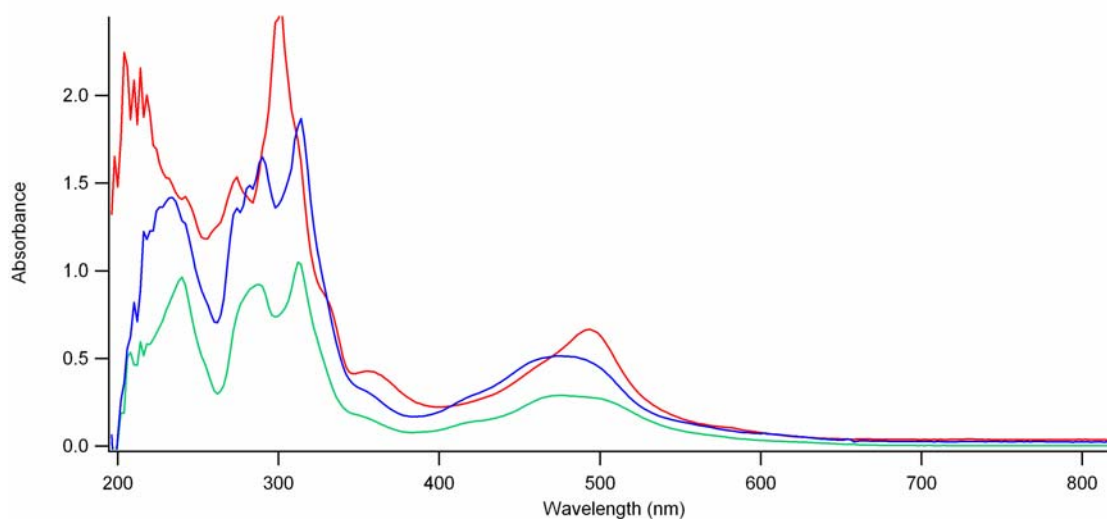


Figure 2.7. UV-VIS spectra of three ruthenium sensitizers in acetonitrile. **Red** trace is $\text{Ru}(\text{trpy})(\text{tfmbpy})(\text{im})^{2+}$, $\lambda_{\text{max}} = 494$ nm. **Green** trace is $\text{Ru}(\text{Cl-trpy})(\text{bpy})(\text{im})^{2+}$, $\lambda_{\text{max}} = 480$ nm. **Blue** trace is $\text{Ru}(\text{trpy})(\text{bpy})(\text{im})^{2+}$, $\lambda_{\text{max}} = 475$ nm.

Absorption measurements were made on the three compounds in acetonitrile (**Figure 2.7**). The peaks around the 470–500 nm region were assigned metal-to-ligand charge transfers (MLCTs) from the t_{2g} orbitals to the π^* of the bpy and trpy analog

ligands. The sharper peaks at 300–350 nm were assigned as the π to π^* of the bpy and trpy ligands.

There is an expected red shift resulting from the installation of the π^* energy-lowering electron-withdrawing groups onto the ligands. Installation of the trifluoromethyl groups on bpy shifts the MLCT more than the chloro on the trpy ligand.

This trend manifests itself in the fluorescence spectra as well. The $[\text{Ru}(\text{trpy})(\text{tfmbpy})(\text{im})](\text{PF}_6)_2$ emission was observed at 725 nm (**Figure 2.8**), extremely red-shifted from the $[\text{Ru}(\text{Cl-trpy})(\text{bpy})(\text{im})](\text{PF}_6)_2$ emission, which was observed at 700 nm. Still bluer than that is the emission of the unmodified $[\text{Ru}(\text{trpy})(\text{bpy})(\text{im})](\text{PF}_6)_2$, which can be found at 695 nm.

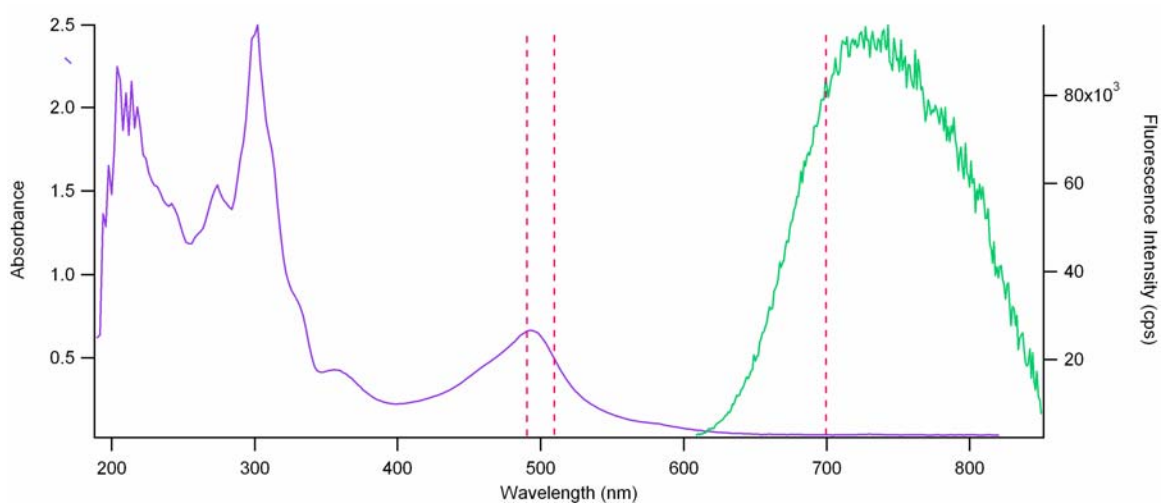


Figure 2.8. Absorption (purple) and emission (green) spectra of $[\text{Ru}(\text{trpy})(\text{tfmbpy})(\text{im})](\text{PF}_6)_2$ in acetonitrile. Wavelengths of interest are highlighted with the hashed pink line. The photosensitizer will be excited at either 490 nm or 510 nm, and Ru^{2+} will be monitored at the other, with the use of a long-pass filter. $^*\text{Ru}^{2+}$ will be monitored at 700 nm.

The cyclic voltammetry (CV) measurements exhibited similar (and the hoped for) trend (**Figure 2.9**). Due to solubility issues, CV measurements had to be executed in

acetonitrile. The tfmbpy clearly accomplishes the goal of raising the potential of the ruthenium dye (**Table 2.3**).

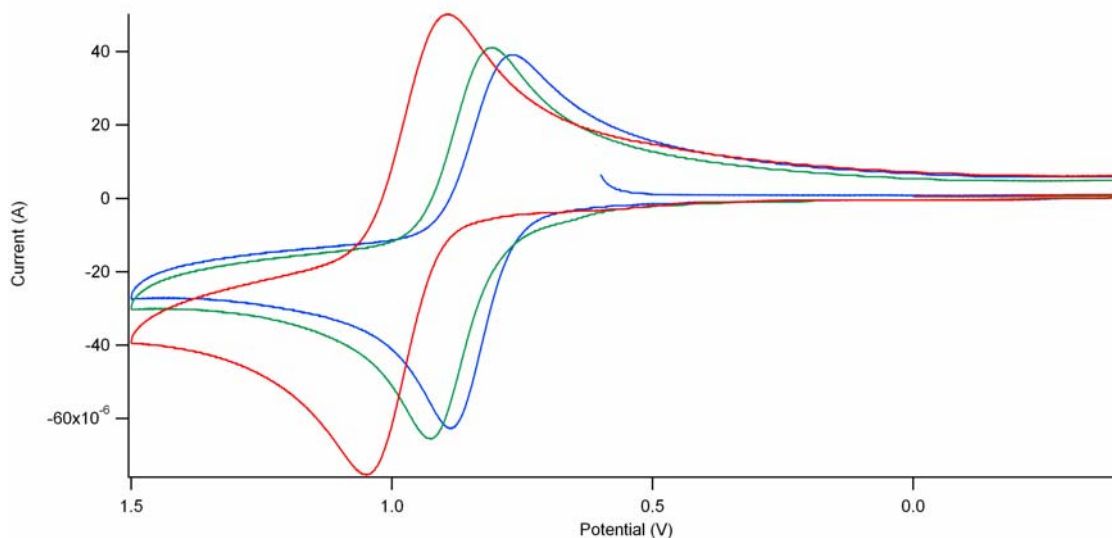


Figure 2.9. Cyclic voltammograms of three ruthenium sensitizers. Red trace is $\text{Ru}(\text{trpy})(\text{tfmbpy})(\text{im})^{2+}$. Green trace is $\text{Ru}(\text{Cl-trpy})(\text{bpy})(\text{im})^{2+}$. Blue trace is $\text{Ru}(\text{trpy})(\text{bpy})(\text{im})^{2+}$.

| molecule | E (V v. Ag/AgNO ₃ , in ACN) |
|--|--|
| $\text{Ru}(\text{trpy})(\text{bpy})(\text{im})$ | 0.83 |
| $\text{Ru}(\text{Cl-trpy})(\text{bpy})(\text{im})$ | 0.87 |
| $\text{Ru}(\text{trpy})(\text{tfmbpy})(\text{im})$ | 0.97 |

Table 2.3. Reduction potentials of three ruthenium sensitizers. Measured at room temperature in acetonitrile. Silver/silver nitrate reference electrode

The lifetime of the excited state of $^*[\text{Ru}(\text{trpy})(\text{tfmbpy})(\text{im})]^{2+}$ was found to be approximately 33 ns in water. The reduction potential of the $\text{Ru}^{2+/+}$ couple was also measured. A modified Latimer diagram was constructed from the data obtained (**Figure 2.10**). Because **Figure 2.4** was constructed on potentials v. Ag/AgCl, it is not fair to compare the two values. However, it can be observed, based on the results described in the later chapters, that $^*[\text{Ru}(\text{trpy})(\text{tfmbpy})(\text{im})]^{2+}$ does not have as high a potential as

*Re⁺ with either phen or dmp as ligand, and the Ru^{3+/2+} couple does not have as high a potential as Re^{2+/+}.

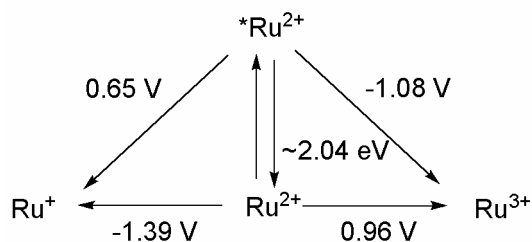


Figure 2.10. Modified Latimer diagram of Ru(trpy)(tfmbpy)(im). Constructed from values obtained in acetonitrile, using a Ag/AgNO₃ reference electrode

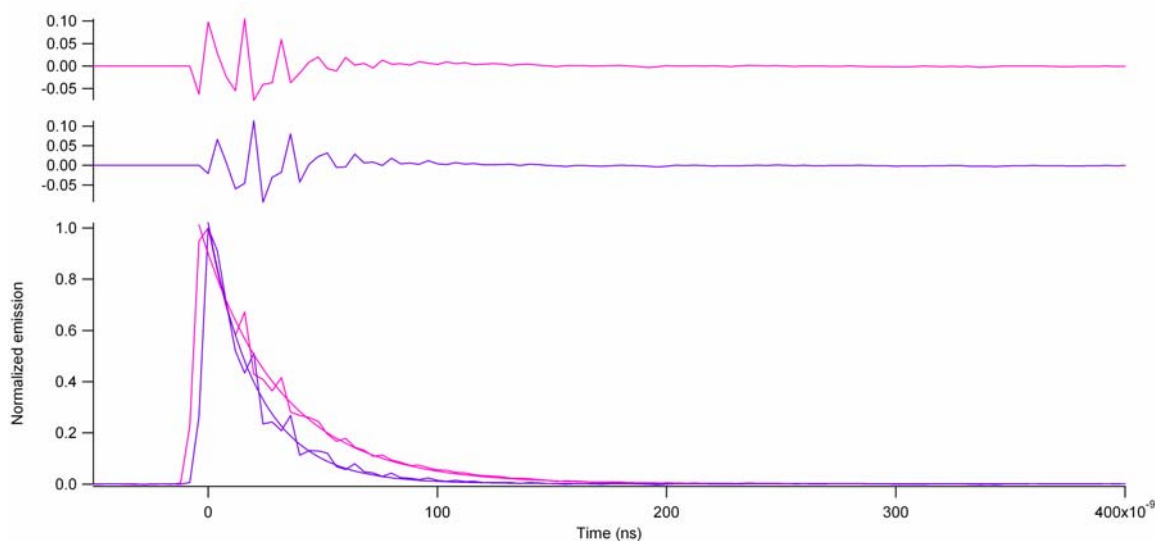


Figure 2.11. Emission data: Ru(trpy)(tfmbpy)(im)²⁺ without (pink) and with (purple) quencher. 25 μM [Ru(trpy)(tfmbpy)(im)](PF₆)₂ in 50 mM NaP_i, pH 7.7, 80 mM methyl viologen. λ_{ex} = 510 nm, λ_{em} = 700 nm. τ = 33 ns without quencher, 21 ns with quencher

Because it seemed likely that Ru³⁺ would be needed to be accessed during photochemical measurements, quenchers were tested. *[Ru(trpy)(tfmbpy)(im)]²⁺ has a disappointingly short lifetime, so there was a worry that the excited state would not live long enough for the intermolecular quench to occur. Indeed, Ru(NH₃)₆²⁺ and lower (< 50

mM) concentrations of methyl viologen did not succeed in oxidizing $^*Ru^{2+}$. However, 80 mM methyl viologen was found to accomplish the desired goal (**Figure 2.11**).

There was a small disadvantage to using methyl viologen, however; in its reduced state, methyl viologen absorbs in the 600 nm region, which complicates transient absorption studies done to probe Cu^{2+} generation. It was soon found, however, that the labeled proteins did not need to for the ruthenium to be oxidized to the Ru^{3+} state in order for interesting kinetics to occur. Further experiments with methyl viologen as a quencher were discontinued.

Rhenium

Despite its optical inactivity, rhenium's high potential was too much of a benefit to ignore. Systems were still pursued utilizing $[Re(dmp)(CO)_3]^+$. This proved to be a wise decision: the two successful hopping systems utilize Re^+ . Brian S. Leigh was generous enough to provide the $[Re(dmp)(CO)_3(H_2O)]OTf$ needed for protein labeling, and Dr. Angel J. Di Bilio provided the model compound $[Re(dmp)(CO)_3(im)]OTf$ for control measurements. Procedures to make both species can be found in Dr. Jeremiah E. Miller's thesis.¹³

Azurin

Site-Directed Mutagenesis & Expression of Mutants

As discussed above, a few mutations have to be made to *Pseudomonas aeruginosa* azurin to facilitate successful hopping experiments. The surface His83 is changed into a Gln, and resident Tyr72, Tyr108, Trp48 are changed into Phe. This

mutant is misleadingly but still appropriately named the All-Phe mutant (**Figure 2.12**). All further site-directed mutagenesis was executed on the plasmid carrying the All-Phe azurin mutant. Established protocols were assiduously followed;¹³ expression of desired mutants was achieved with little difficulty. Yuling Sheng executed site-directed mutagenesis and expressed most of the mutants needed for the studies described.

```

          10          20          30          40          50
AECSVDIQGNDQMQFNTNAITVDKSCKQFTVNLSHPGNLPKNVMGHNFVLSTAADMQ

          60          70          80          90          100          110
GVVTDGMASGLDKDFLKPDDSRVIAQTKLIGSGEKDSVTFDVSKLKEGEQFMFFCTF

          120
PGHSALMKGTLTLK

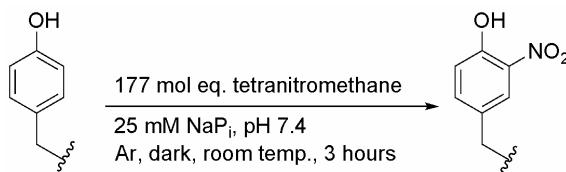
```

Figure 2.12. Sequence of All-Phe azurin. The mutations to the wild type are highlighted; H83Q in red, and W48F, Y72F, and Y108F are highlighted in blue.

Nitration of Tyrosine

Tyrosine was inserted into the sites of interest using site-directed mutagenesis. Previously established nitration protocols were followed, in which the protein was exposed to tetranitromethane. Protocols were obtained from Bert Tsunyin Lai, Dr. Jennifer C. Lee, and Prof. Michele McGuirl (University of Montana). UV-VIS spectra were obtained to confirm nitration of the tyrosine (**Figure 2.13**). The first mutant on which nitration was attempted was H107/Y110/Az(Cu²⁺). This was an unfortunate selection, as the tyrosine was unreactive to tetranitromethane at this site, and proved to remain so in all future attempts, even after a successful protocol had been developed. A strategy was undertaken to unfold the protein, nitrate the residue, and allow the protein to refold. The strategy with complete unfolding of the protein was unsuccessful; while it appeared that the tyrosine had been nitrated, the protein would not refold. It has been

previously observed that tetranitromethane oxidizes cysteines, resulting in disulfide bridges and sulfinic acids.²⁹ It is likely that unfolding the protein exposes the copper-ligating Cys112 and possibly the disulfide bridging Cys3 and Cys26 to oxidations that disrupt the protein's structure. To circumvent this problem, unfolding studies were carried out to probe the possibility of loosening the protein structure just enough to expose the tyrosine for nitration, but not lose copper ligation. These experiments are listed and discussed below in the next section; the conditions that seemed optimal for nitration trials were either 40% methanol or 3 M urea. Both conditions were attempted; the reaction in methanol was not at all successful, and the reaction run in 3 M urea resulted in a miniscule yield of the desired product, the greater percentage of product being the oxidized unfolded azurin.



Scheme 2.3. Nitration of tyrosine

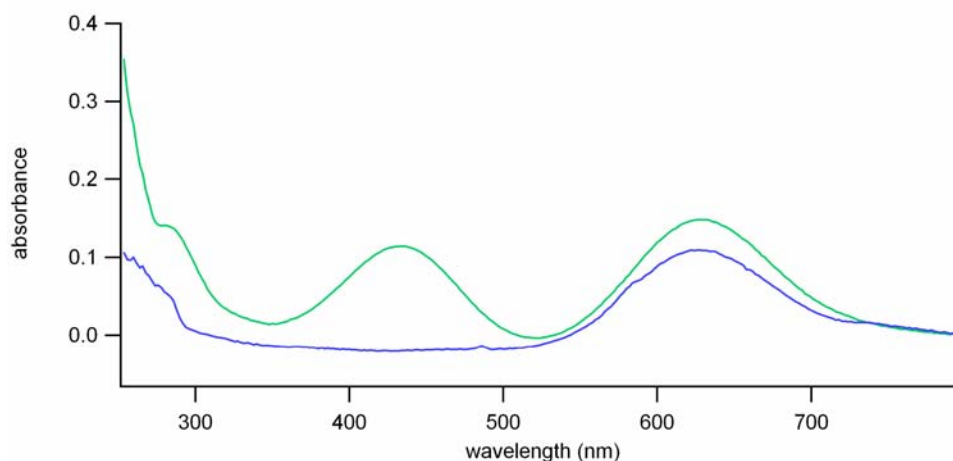


Figure 2.13. UV-VIS of successful nitration. **Blue** trace is H107/Y109/Az(Cu²⁺) in 25 mM NaPi. **Green** trace is H107/YNO₂109/Az (Cu²⁺) in 25 mM DEA, pH 8.8.

When nitration was attempted on H107/Y109/Az(Cu²⁺) without any denaturants, the tyrosine was nitrated without any difficulty. It is likely that the tyrosine at the 110 site was simply not exposed enough to react. The protocol utilized to nitrate at the 109 site was also utilized to successfully nitrate at the 122 site (**Scheme 2.3**).

Routinely, the protein was nitrated prior to labeling, for labeling was the lower-yielding reaction of the two. Once nitrated, the protein would be purified using anion exchange chromatography.

It was important to purify either the nitrated unlabeled protein or the nitrated labeled protein using cation-exchange chromatography. Purification using cation-exchange chromatography at either stage yielded two major products; one green in color, and one blue, both of the same mass. The blue product is the expected and desired mutant; at pH 4.52, the nitrotyrosine should be protonated, and thus not absorb at 434 nm. The green product was pursued and studied, but no productive or interesting results came of the studies; it remains unclear what, exactly, it is, though it is conjectured that it is a side-product of the nitration reaction with an altered protein structure.

Once the purity of the sample was ascertained by mass spectrometry, the protein was then ready for labeling reactions.

Unfolding Studies

Unfolding studies were carried out in varying concentrations of methanol and urea in the hopes of finding a concentration of denaturant that would perturb secondary structure, but leave copper binding undisturbed. The copper coordination was monitored by UV-VIS spectroscopy and the extent of secondary structure was measured using

circular dichroism (CD). The resulting unfolding conditions would be employed in a nitration reaction, so the buffer used in these studies was the 50 mM sodium phosphate, pH 8.0 that was to be used in the reaction. The mutant used for these studies was H107/Y110/Az(Cu²⁺).

The results of the experiments done with methanol are shown in **Figures 2.14–2.16**. Measurements were made on eleven samples of azurin, with increasing concentrations of methanol, every 10% from 0 to 100%. The UV-VIS spectra indicate that the protein is aggregating with increased concentrations; the baseline is migrating upwards with every sample. At around 80% methanol, solubility became a problem. The measurement at 40% methanol, indicated in **Figure 2.14** with a solid line, shows the copper center intact, as well as minor aggregation. The CD spectra show strange incongruity, but the measurement at 40% methanol clearly displays the predicted behavior; less secondary structure compared to wild type. 40% methanol was determined to be the optimal concentration of methanol to achieve the desired effect on the protein.

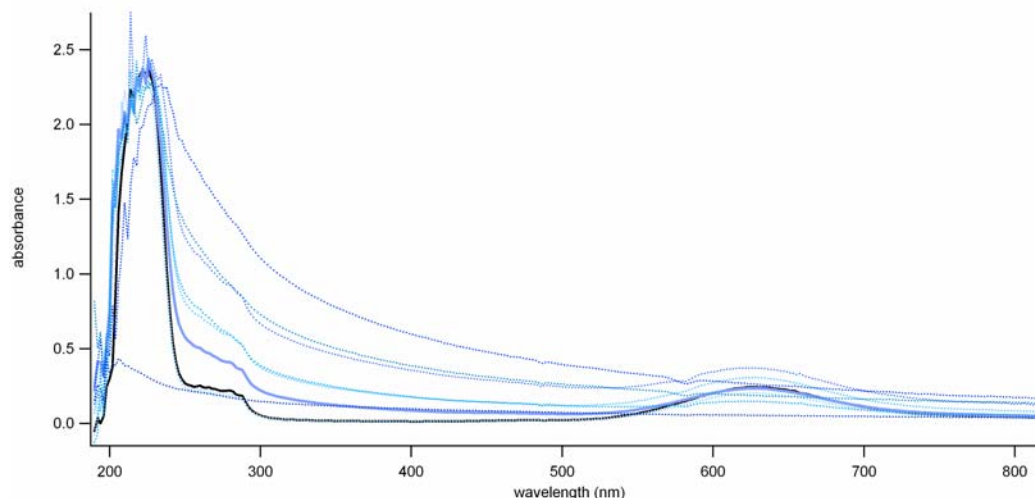


Figure 2.14. UV-VIS spectra of azurin in increasing concentrations of methanol. $4 \mu\text{M}$ H107/Y110/Az(Cu^{2+}) in 50 mM NaP_i , pH 8 in 1 mm path length cuvette. Data for increasing concentrations of methanol (0–100% v/v, a sample at each 10% increment) are displayed in gradient of shades; the lightest shades are of the lesser methanol concentrations, the darker are for the more concentrated. The control measurement without methanol is indicated in black. The spectrum at 40% methanol is solid blue.

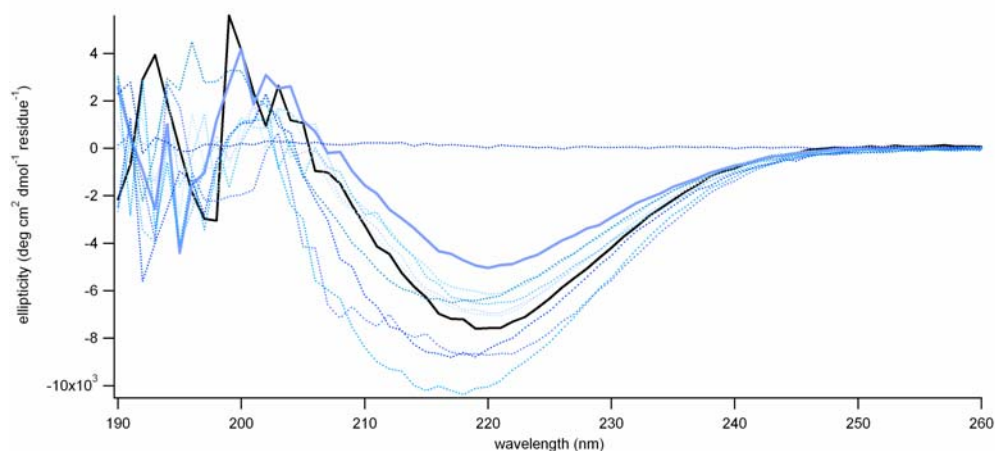


Figure 2.15. CD spectra of azurin in increasing concentrations of methanol. $4 \mu\text{M}$ H107/Y110/Az(Cu^{2+}) in 50 mM NaP_i , pH 8 in 1 mm path length cuvette. Data for increasing concentrations of methanol (0–100% v/v, a sample at each 10% increment) are displayed in gradient of shades; the lightest shades are of the lesser methanol concentrations, the darker are for the more concentrated. The control measurement without methanol is indicated in black. The spectrum at 40% methanol is solid blue.

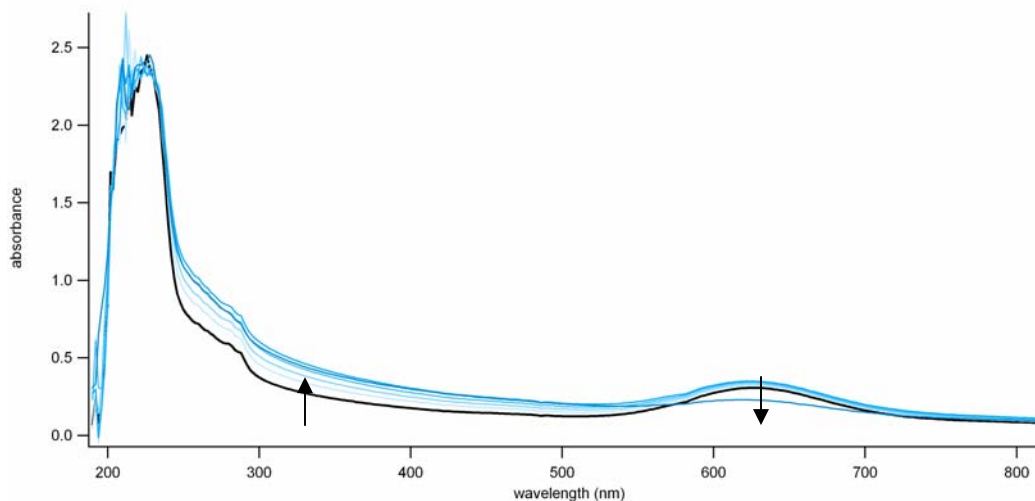


Figure 2.16. UV-VIS of azurin in 50% methanol over time. 4 μM H107/Y110/Az(Cu^{2+}) in 50% methanol/50 mM NaP_i , pH 8 in 1 mm path length cuvette. Spectra were taken immediately, 2, 5, 10, 30, and 270 minutes after the sample was made; darker shades for more time elapsed.

The 50% methanol/50% buffer sample was monitored to check for denaturation over time; while aggregation occurred over the span of the first 30 minutes, diminished binding of the copper center was not evident. Four and a half hours later, aggregation and unfolding of the Cu^{2+} center has rendered the sample useless. While these experiments were not executed on the 40% methanol sample, it is clear that there is a limit to the reaction time; it would defeat the purpose of finding optimal conditions if these optimal conditions also destroyed the reactants.

The results of the experiments done with urea are shown in **Figures 2.17–2.22**. Measurements were made on nine samples of azurin, with increasing concentrations of urea, every 1 M increment from 0 to 8 M. These experiments yielded more aesthetically pleasing and predictable results; the UV-VIS reveals no aggregation; simply deterioration structure and copper binding site. The CD measurements also demonstrate the same aesthetically pleasing predictability. It was found, however, that the samples had not

been given enough time to equilibrate before measurements; the measurements were therefore repeated in 24 hours.

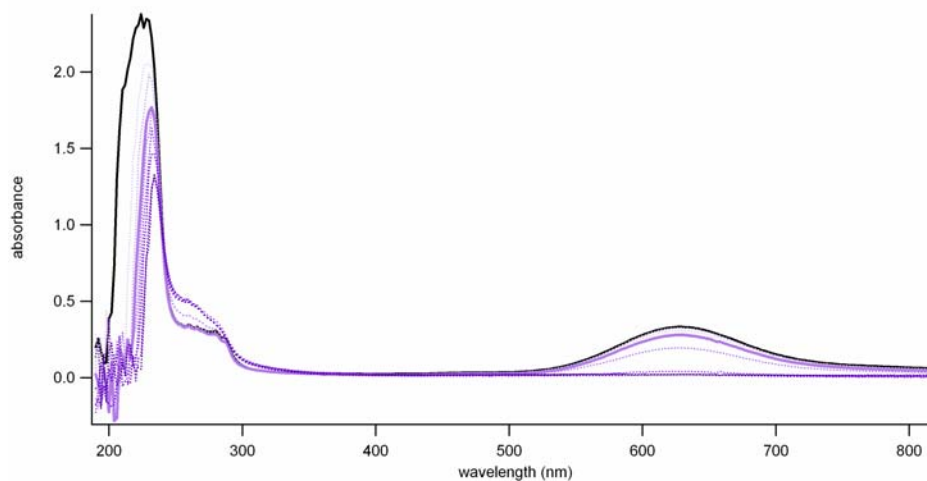


Figure 2.17. UV-VIS spectra of azurin in increasing concentrations of urea. 5 μM in H107/Y110/Az(Cu^{2+}) in 50 mM NaP_i , pH 8 in 1 mm path length cuvette. Data for increasing concentrations of urea (0–8 M, a sample at each 1 M increment) are displayed in gradient of shades; the lightest shades are of the lesser urea concentrations, the darker are for the more concentrated. The control measurement without urea is indicated in black. The spectrum at 3 M urea is solid purple.

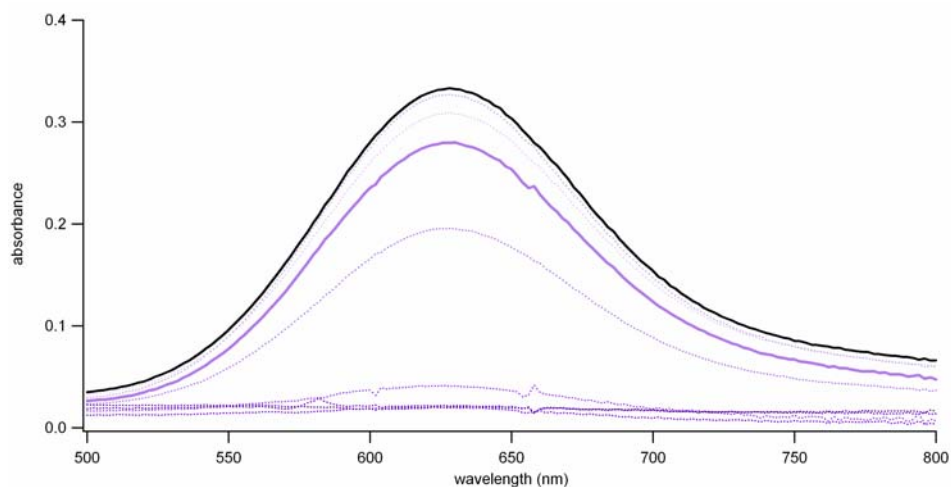


Figure 2.18. Zoom in of 500–800 nm region of **Figure 2.17**. 5 μM H107/Y110/Az(Cu^{2+}) in 50 mM NaP_i , pH 8 in 1 mm path length cuvette. Data for increasing concentrations of urea (0–8 M, a sample at each 1 M increment) are displayed in gradient of shades; the lightest shades are of the lesser urea concentrations, the darker are for the more concentrated. The control

measurement without urea is indicated in black. The spectrum at 3 M urea is solid purple.

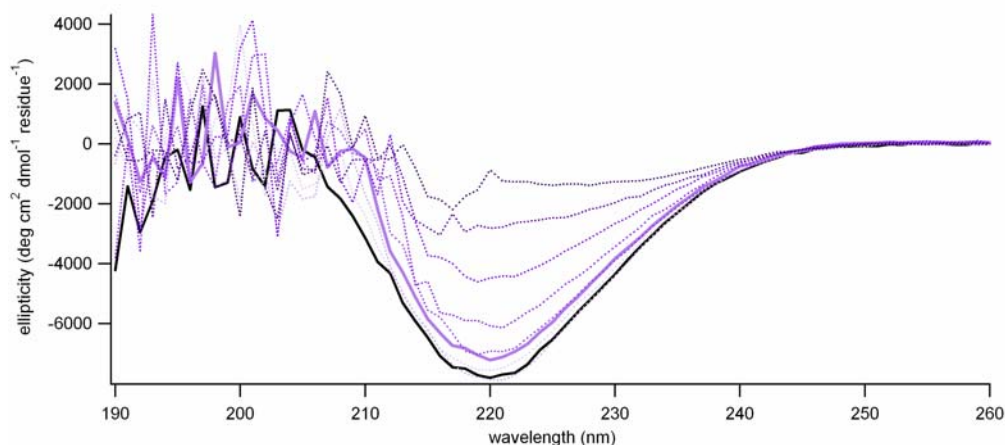


Figure 2.19. CD spectra of azurin in increasing concentrations of urea. 5 μM H107/Y110/Az(Cu^{2+}) in 50 mM NaP_i , pH 8 in 1 mm path length cuvette. Data for increasing concentrations of urea (0–8 M, a sample at each 1 M increment) are displayed in gradient of shades; the lightest shades are of the lesser urea concentrations, the darker are for the more concentrated. The control measurement without urea is indicated in black. The spectrum at 3 M urea is solid purple.

Measurements made after equilibration demonstrate a clear choice for optimal conditions; the UV-VIS spectra reveal that the copper center has deteriorated in samples with 4 M or higher concentrations of urea (**Figures 2.20–2.21**). The CD spectra indicate that at concentrations lesser than 3 M, azurin retains much of its secondary structure (**Figure 2.22**). Given these observations, 3 M urea (after the protein has been allowed to equilibrate in the solution) seems to be at the perfect point, where the copper center maintains its integrity and the secondary structure is being compromised to only a minor degree.

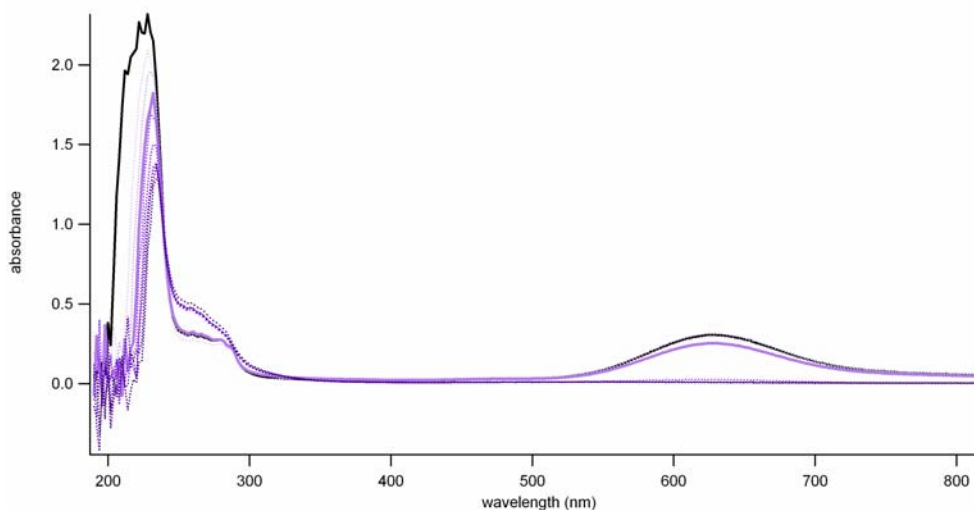


Figure 2.20. UV-VIS spectra of azurin in increasing concentrations of urea, 24 hours. $5 \mu\text{M}$ H107/Y110/Az(Cu^{2+}) in 50 mM NaP_i , pH 8 in 1 mm path length cuvette. Data for increasing concentrations of urea (0–8 M, a sample at each 1 M increment) are displayed in gradient of shades; the lightest shades are of the lesser urea concentrations, the darker are for the more concentrated. The control measurement without urea is indicated in black. The spectrum at 3 M urea is solid purple.

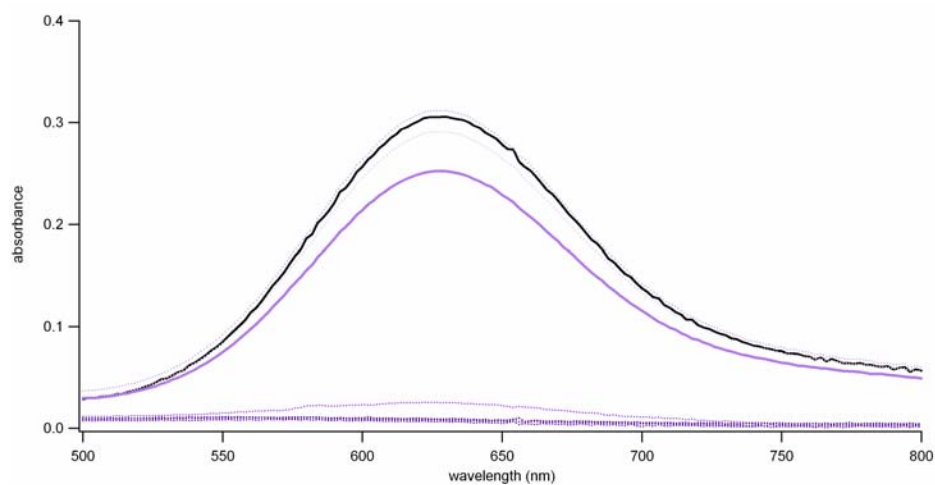


Figure 2.21. Zoom in of 500–800 nm region of **Figure 2.20**. $5 \mu\text{M}$ H107/Y110/Az(Cu^{2+}) in 50 mM NaP_i , pH 8 in 1 mm path length cuvette. Data for increasing concentrations of urea (0–8 M, a sample at each 1 M increment) are displayed in gradient of shades; the lightest shades are of the lesser urea concentrations, the darker are for the more concentrated. The control measurement without urea is indicated in black. The spectrum at 3 M urea is solid purple.

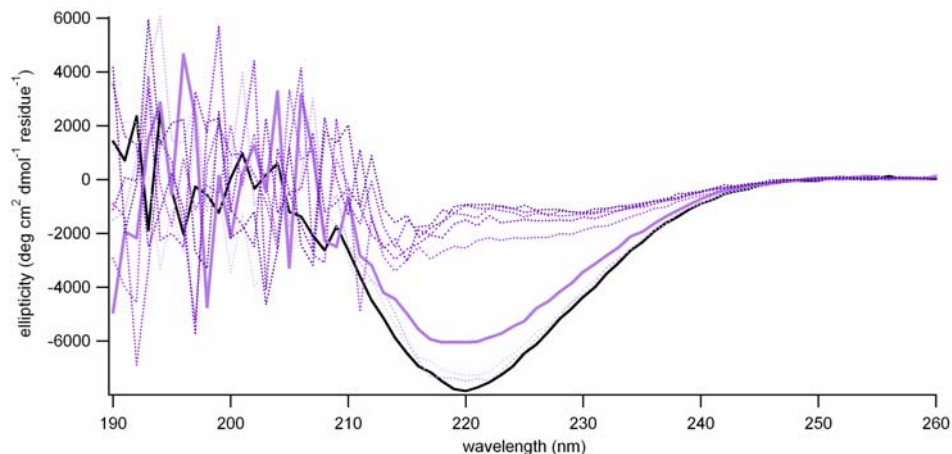
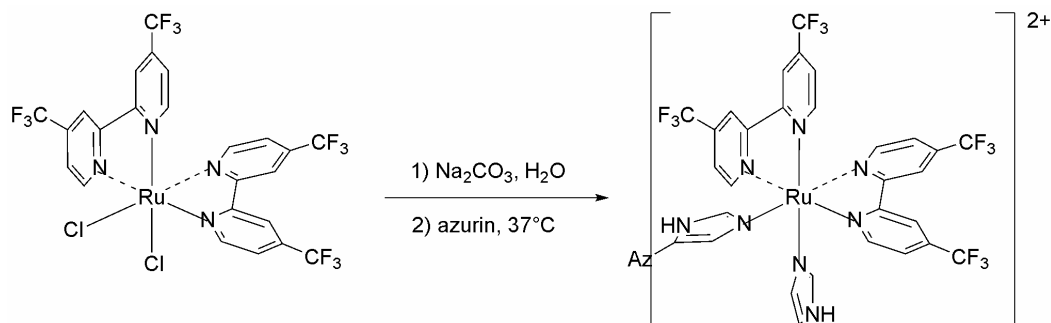
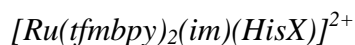


Figure 2.22. CD spectra of azurin in increasing concentrations of urea, 24 hours. 5 μ M H107/Y110/Az(Cu^{2+}) in 50 mM NaP_i , pH 8 in 1 mm path length cuvette. Data for increasing concentrations of urea (0–8 M, a sample at each 1 M increment) are displayed in gradient of shades; the lightest shades are of the lesser urea concentrations, the darker are for the more concentrated. The control measurement without urea is indicated in black. The spectrum at 3 M urea is solid purple.

Metal-Labeled Azurin



Scheme 2.4. Generation of $\text{Ru}(\text{tfmbpy})_2\text{CO}_3$ and installation onto azurin

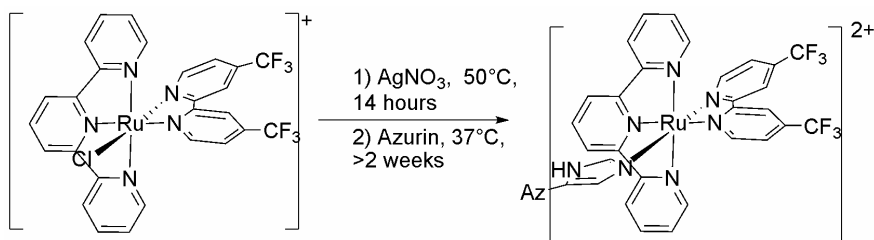
Installing $[\text{Ru}(\text{tfmbpy})_2(\text{im})]^{2+}$ label onto the protein proved to be too difficult. Traditionally, the $\text{Ru}(\text{bpy})_2\text{CO}_3$ species is made from $\text{Ru}(\text{bpy})_2\text{Cl}_2$ in preparation for the labeling reaction (**Scheme 2.4**).³⁰⁻³² The carbonate is a labile leaving group and allows for facile generation of the $\text{Ru}(\text{bpy})_2(\text{H}_2\text{O})_2^{2+}$ intermediate, which attaches onto the

protein. The $\text{Ru}(\text{tfmbpy})_2\text{CO}_3$ was a difficult species to generate, no doubt owing the unreactivity of the $\text{Ru}(\text{tfmbpy})_2\text{Cl}_2$ complex.

Beyond this complication, another disadvantage of this labeling system was recognized: previous flash-quench experiments with $[\text{Ru}(\text{bpy})_2(\text{im})(\text{HisX})]^{2+}$ -labeled protein indicated that upon excitation, the imidazole ligand was found to exchange with water.³³ This might not have necessarily been the outcome of the studies with the electron-deficient tfmbpy-substituted analog, but this possibility, coupled with the unreactivity of complex certainly rendered $[\text{Ru}(\text{tfmbpy})_2(\text{im})(\text{HisX})]^{2+}$ less exciting a label prospect.



The established labeling protocol involves stripping the chloride away from $[\text{Ru}(\text{trpy})(\text{tfmbpy})\text{Cl}]^+$ and precipitating silver chloride, leaving the aquo intermediate ready for substitution onto protein. While previously reported labelings with $[\text{Ru}(\text{trpy})(\text{bpy})]^{2+}$ took a mere 24 hours at room temperature,²⁸ the unreactive nature of the $[\text{Ru}(\text{trpy})(\text{tfmbpy})]^{2+}$ required a two-week, 37°C incubation time (**Scheme 2.5**). Nonetheless, a moderate amount of labeled protein could be isolated, and so the label and protocol were used to modify proteins in various sites.



Scheme 2.5. Generation of $[\text{Ru}(\text{trpy})(\text{tfmbpy})(\text{H}_2\text{O})]\text{NO}_3$ followed by installation onto azurin

Labeled azurin was separated from unlabeled by running the product mixture of labeled and unlabeled protein sample through a chelating column. The labeled protein product was confirmed by UV-VIS spectroscopy (**Figure 2.23**). It was further purified by ion exchange chromatography, checked for purity using mass spectrometry, and stored in the dark at 4°C in 25 mM NaOAc, pH 4.52. Prior to laser spectroscopy measurements, stored labeled protein was once more purified using the chelating column and ion exchange chromatography. Mass spectrometry and UV-VIS spectroscopy was carried out on the sample to confirm sample purity.

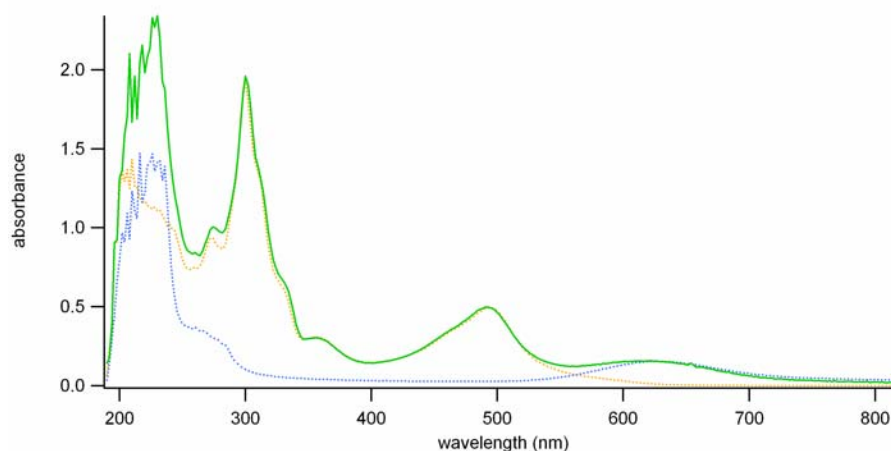


Figure 2.23. UV-VIS spectrum of $[\text{Ru}(\text{trpy})(\text{tfmbpy})]^{2+}$ -labeled azurin. **Green** trace is $\text{Ru}(\text{trpy})(\text{tfmbpy})(\text{H107}/\text{Y108}/\text{Az})(\text{Cu}^{2+})$. **Blue** trace is $\text{H107}/\text{Y108}/\text{Az}(\text{Cu}^{2+})$. **Orange** trace is $[\text{Ru}(\text{trpy})(\text{tfmbpy})(\text{im})](\text{PF}_6)_2$. All samples were made in 25 mM NaP_i , pH 7.2.



Protocols to install rhenium labels onto proteins are very well established,²⁴ and were followed accordingly. A different approach to purification was taken; a different chelating column was used to separate unlabeled from labeled protein, and while the column remained the same, a different gradient was used in cation-exchange

chromatography. For the nitrotyrosine mutants, an anion-exchange chromatography was executed after. Purity of the sample was ascertained by mass spectrometry. If the sample was stored before laser spectroscopy experiments, chelating, cation-exchange, and anion-exchange chromatography would once more be executed to ensure purity of the sample.

Labeled Proteins

| Protein | Chapter |
|---|---------|
| Re124/W122/Cu ²⁺ | 3 |
| Ru124/W122/Cu ²⁺ | 4 |
| Ru124/W122/Zn ²⁺ | 4 |
| Ru124/F122/Zn ²⁺ | 4 |
| Ru124/YNO ₂ 122/Cu ²⁺ | 4 |
| Re124/YNO ₂ 122/Cu ²⁺ | 4 |
| Ru126/W122/Cu ²⁺ | 4 |
| Re126/W122/Cu ²⁺ | 4 |
| Re126/F122/Cu ²⁺ | 4 |
| Ru83/F48/Cu ²⁺ | 5 |
| Ru83/Y48/Cu ²⁺ | 5 |

Table 2.4. Labeled proteins studied in this dissertation, and the chapters that discuss them. [Ru(trpy)(tfmbpy)]²⁺ labeling is abbreviated as Ru and [Re(dmp)(CO)₃]⁺ labeling is abbreviated Re.

2.4 CONCLUSIONS

Three high-potential ruthenium sensitizers were synthesized in the pursuit of a photosensitizer that was both high-potential and optically active. This was accomplished through the use of installing electron-withdrawing groups onto the ligand framework. Difficulties were encountered with the initially pursued [Ru(tfmbpy)₂(im)(HisX)]²⁺ when it was found that substitution onto the protein was not straightforward. Utilizing the 3-2-1 architecture of [Ru(trpy)(bpy)(HisX)]²⁺ proved to be more successful.

$[\text{Ru}(\text{trpy})(\text{tfmbpy})(\text{HisX})]^{2+}$ was proven to be of high potential and could be installed onto the protein.

Site-directed mutagenesis and protein expression garnered desired mutants. To gain the nitrotyrosine moiety, the tyrosine mutant was first expressed, and established protocol was followed to nitrate the residue using tetranitromethane. The position of the tyrosine was shown to be extremely important in determining the success of the reaction. Unfolding studies were executed on a mutant of azurin to probe if unfolding the protein would assist in exposing the residue for nitration reactions; it was found that unfolding, even to a small degree, still allows destructive side reactions.

Protocols to label and purify hopping systems are outlined; only minor revisions had to be made to established protocol to achieve the desired results. In total, eleven azurin mutants were labeled, characterized, and studied throughout the course of this dissertation, the results of which are described in the following chapters.

2.5 EXPERIMENTALS

Materials

2-Chloro-4-(trifluoromethyl)pyridine was purchased from Matrix Scientific. All other reagents were purchased from Aldrich. Dry THF was obtained from the solvent columns. Absolute EtOH was obtained from Aaper. Other reagent-grade solvents were purchased from VWR and were used without further purification.

Resources and Instrumentation

Prior to June 2007, DNA sequencing was obtained from the Caltech Sequence and Structure Analysis Facility. After June 2007, the sequences were obtained from Laragen. Mass spectrometry on small molecules was carried out by Dr. Lionel Cheruzel or Dr. Mona Shahgholi at the mass spectrometry facility at Caltech. Mass spectrometry on protein samples were carried out at the Beckman Institute Protein/Peptide Micro Analytical Laboratory by Dr. Jie Zhou.

UV-VIS spectra were taken on an Agilent 8453 UV-VIS spectrometer. Steady-state fluorescence measurements were made using a Fluorolog Model FL3-11 fluorometer equipped with a Hamamatsu R928 PMT. ¹H-NMR spectra were obtained on a Varian Mercury spectrometer operating at 300 MHz in Caltech's NMR Facility. CD spectra were taken on an Aviv 62ADS spectropolarimeter (Aviv Associates, Lakewood, NJ). CV measurements were made using a Model 660 Electrochemical Workstation (CH-Instrument, Austin, TX). Laser spectroscopy, unless otherwise specified, was executed using the Nanosecond-I setup in the Beckman Institute Laser Resource Center.

Synthesis & Characterization of Ruthenium Model Compounds

$\text{Ru}(\text{trpy})\text{Cl}_3$ ³⁴, $[\text{Ru}(\text{trpy})(\text{bpy})(\text{im})](\text{PF}_6)_2$ ³⁵ were synthesized following previously reported protocols.

4,4'-bis(trifluoromethyl)-2,2'-bipyridine (tfmbpy)

A literature preparation was modified to obtain this ligand.³⁶

Under argon, Ni(Ph₃P)₂Cl₂ (3.92 g, 6 mmol), zinc dust (1.96 g, 30 mmol), and Et₄Ni (5.14 g, 20 mmol) were added to a 100 mL Schlenck flask equipped with a stir bar. Dry THF (40 mL) was added and the mixture was stirred at room temperature for 30 minutes. The mixture turned dark red. In a second 25 mL round-bottom flask and under argon, 2-chloro-4-trifluoromethylpyridine was added to 10 mL dry THF. The chloro-pyridine solution was added to the reaction pot via cannula transfer. The reaction was heated for three days at 60°C with stirring to yield a dark brown-black solution. The flask was then cooled to room temperature and added into 200 mL aqueous ammonia and extracted into 200 mL of a 1:1 mixture of benzene and diethyl ether. The aqueous phase was washed with 1:1 benzene/ether mixture (100 mL, 2 times). The combined organic layers were then washed with water and brine, dried over MgSO₄, and filtered. The mixture was then concentrated down to yield a brown oil. Subsequent column chromatography performed on silica gel with 20% dichloromethane/hexanes (R_f = 0.2) yielded a white powder. The ¹H-NMR matches that given in the literature. Yield: 1.14 g (39%).

Ru(tfmbpy)₂Cl₂·2H₂O

The synthesis of this compound was modified from a preparation taken from literature.³⁷

RuCl₃·2.5 H₂O (169 mg, 0.67 mmol), tfmbpy (394 mg, 1.35 mmol), LiCl (189 mg, 4.47 mmol), and 1.1 mL DMF were added to a two dram vial equipped with a stir bar. The vial was sealed with a Teflon screw-cap and the reaction was stirred at reflux for 24 hours. The reaction mixture was then cooled to room temperature, added to 50 mL

reagent-grade acetone, and stored at -10°C overnight. Filtering yielded a red-purple solution and dark purple powder. The powder was washed three times with water (5 mL) and three times with diethyl ether (5 mL), and dried on a vacuum line. Yield: 252 mg (47%). The $^1\text{H-NMR}$ was checked against literature.

[Ru(tfmbpy)₂(im)₂](PF₆)₂

The synthesis of this compound was modified from a preparation taken from literature.³⁷

$\text{Ru}(\text{tfmbpy})_2\text{Cl}_2 \cdot 2.5 \text{ H}_2\text{O}$ (200 mg, 0.25 mmol), AgClO_4 (156 mg, 0.75 mmol), and 25 mL reagent-grade argon-sparged acetone were added to a 100 mL round-bottom flask equipped with a stir bar. The mixture was stirred at room temperature overnight, and the AgCl precipitate was removed by filtration. The mixture was added to a 50 mL round-bottom flask with stir bar. Imidazole (68 mg, 1 mmol) was added to the mixture under argon. A condenser was then attached and sealed off with a septum. The reaction was heated at reflux with stirring for 3 days. After cooling the reaction to room temperature, the mixture was concentrated to approximately one-third of its original volume and added to 17 mL water. NH_4PF_6 was added to precipitate out the dark purple powder product. The powder was isolated by filtration and washed with a generous amount of water and diethyl ether. The product was then dried on the vacuum line. Yield: 123 mg (44%). $^1\text{H-NMR}$ (d_6 -DMSO), δ : 9.37 (s, 2H), 9.28 (s, 2H), 9.19 (d, 2H, $J = 6 \text{ Hz}$), 8.27 (d, 2H, $J = 6 \text{ Hz}$), 8.20 (dd, 2H, $J = 6.6 \text{ Hz}$, $< 1 \text{ Hz}$), 7.81 (s, 2H), 7.73 (dd, 2H, 6.6 Hz , $< 1 \text{ Hz}$), 7.30 (s, 1H), 6.71 (s, 1H).

[Ru(trpy)(tfmbpy)Cl]Cl

A literature preparation was modified for the synthesis of this compound.³⁵

Ru(trpy)Cl₃ (200 mg, 0.45 mmol), tfmbpy (133 mg, 0.45 mmol), and LiCl (114 mg, 2.69 mmol) were added to a 100 mL round-bottom flask equipped with a stir bar. 45 mL 75% absolute EtOH/water was added to the flask. Finally, 0.1 mL NEt₃ was added as reductant. The mixture was heated to reflux and stirred for 6 hours. The reaction mixture was filtered while still hot and the filtrate was concentrated down to approximately one-third its original volume. It was then stored at 4°C overnight. The resulting purple-black precipitate was collected by filtration and washed two times with 5 mL portions of 3 N HCl, one time with minimal reagent grade acetone, and three times with 10 mL portions of diethyl ether. Yield: 225 mg (71%). ¹H-NMR (*d*₆-DMSO), δ: 10.34 (d, 1H, 6 Hz), 9.60 (s, 1H), 9.35 (s, 1H), 8.86 (d, 2H, J = 8 Hz), 8.71 (d, 2H, J = 8 Hz), 8.46 (dd, 1H, J = 8 Hz, < 1 Hz), 8.31 (t, 1H, J = 8 Hz), 8.02 (td, 2H, J = 8 Hz, 1 Hz), 7.74 (d, 1H, J = 6 Hz), 7.66 (d, 2H, J = 4.5 Hz), 7.43 (dd, 1H, J = 4.5 Hz), 7.36 (td, 2H, J = 6 Hz, < 1 Hz).

[Ru(trpy)(tfmbpy)(im)](PF₆)₂

[Ru(trpy)(tfmbpy)Cl]Cl (100 mg, 0.143 mmol), AgNO₃ (73 mg, 0.429 mmol), and 14.3 mL water were added to a 25 mL round-bottom flask equipped with a stir bar. The reaction stirred at 50°C for 24 hours. The AgCl precipitate was filtered from the red solution. The solution was added to a 50 mL round-bottom flask equipped with a stir bar. To this solution was added imidazole (48 mg, 0.715 mmol). The reaction was then stirred at reflux for 6 days. The reaction mixture was then cooled, and the AgCl that continued to precipitate at this stage was then removed by filtration. NH₄PF₆ was added

to precipitate the product, a dark red-orange powder. The product was isolated by filtration and washed with ether. Yield: 72 mg (51%). $^1\text{H-NMR}$ (d^6 -DMSO), δ : 9.66 (s, 1H), 9.45 (s, 1H), 8.86 (d, 2H, $J = 8.4$ Hz), 8.75 (m, 3H), 8.342 (m, 2H), 8.15 (td, 2H, $J = 6$ Hz, < 1 Hz), 7.89 (d, 2H, $J = 5.4$ Hz), 7.74 (d, 1H, $J = 5.7$ Hz), 7.50 (m, 3H), 7.23 (s, 1H), 7.03 (s, 1H), 6.04 (s, 1H).

[Ru(trpy)(bpy)Cl]Cl

The method used above on the preparation of $[\text{Ru}(\text{trpy})(\text{tfmbpy})\text{Cl}]\text{Cl}$ was followed for the synthesis of this complex.

The amounts used for this synthesis: $\text{Ru}(\text{trpy})\text{Cl}_3$ (100 mg, 0.23 mmol), bpy (36 mg, 0.23 mmol), LiCl (49 mg, 1.15 mmol), 0.15 mL NEt_3 , and 23 mL 75% EtOH/water. The mixture was stirred at reflux for 24 hours. The product was a metallic black powder. Yield: 72 mg (56%). $^1\text{H-NMR}$ (d_6 -DMSO), δ : 10.1 (d, 1H), 8.89 (d, 1H, $J = 7.5$ Hz), 8.80 (d, 2H, $J = 7.8$ Hz), 8.68 (d, 2H, $J = 8.1$ Hz), 8.62 (dd, 2H, $J = 7.2$ Hz, < 1 Hz), 8.34 (m, 1H), 8.20 (t, 1H, $J = 8.1$ Hz), 8.05 (td, 1H, $J = 6$ Hz), 7.97 (m, 2H), 7.76 (td, 1H, $J = 8$ Hz), 7.60 (d, 2H, $J = 4.8$ Hz), 7.33 (m, 3H), 7.06 (m, 1H).

[Ru(trpy)(bpy)(im)](PF₆)₂

The method used in the preparation of $[\text{Ru}(\text{trpy})(\text{tfmbpy})(\text{im})](\text{PF}_6)_2$ was followed for the synthesis of this complex.

The amounts used for this synthesis: $[\text{Ru}(\text{trpy})(\text{bpy})\text{Cl}]\text{Cl}$ (50 mg, 0.082 mmol), AgNO_3 (42 mg, 0.246 mmol), and 8.2 mL of water were stirred at 50°C overnight. After addition of imidazole (28 mg, 0.41 mmol), the reaction was heated to reflux and stirred

for 24 hours. The product is a dark red-orange solid. Yield: 57 mg (Quantitative Yield).

$^1\text{H-NMR}$ (d_6 -DMSO), δ : 8.95 (d, 1H), 8.78 (m, 5H), 8.52 (d, 1H, $J = 4.8$ Hz), 8.38 (m, 1H), 8.26 (t, 1H), 8.12 (t, 2H, $J = 7$ Hz), 7.93 (m, 2H), 7.81 (d, 2H, $J = 5.1$ Hz), 7.51 (t, 2H, $J = 6.3$ Hz), 7.37 (d, 1H, $J = 5.7$ Hz), 7.18 (m, 2H), 7.0 (s, 1H), 6.02 (s, 1H).

Ru(Cl-trpy)Cl₃

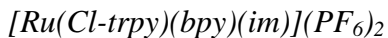
The method used above on the preparation of $\text{Ru}(\text{trpy})\text{Cl}_3$ was followed in the synthesis of this complex.

The amounts used in this synthesis: $\text{RuCl}_3 \cdot 2.5 \text{ H}_2\text{O}$ (253 mg, 1 mmol), Cl-trpy (268 mg, 1 mmol), and 125 mL absolute EtOH. The reaction was stirred at reflux for 6.5 hours. The product is a light brown powder. Yield: 375 mg (72%).

[Ru(Cl-trpy)(bpy)Cl]Cl

The method used above on the preparation of $[\text{Ru}(\text{trpy})(\text{tfmbpy})\text{Cl}]\text{Cl}$ was followed in the synthesis of this complex.

The amounts used in this synthesis: $\text{Ru}(\text{Cl-trpy})\text{Cl}_3$ (200 mg, 0.42 mmol), bpy (131 mg, 0.84 mmol), LiCl (118 mg, 2.8 mmol), 0.1 mL NEt_3 , and 44 mL 75% EtOH/water. This mixture was stirred at reflux for 6 hours. The product was a metallic black powder. Yield: 94 mg (35%). $^1\text{H-NMR}$ (d_6 -DMSO), δ : 10.06 (d, 1H, $J = 5.4$ Hz), 9.09 (s, 2H), 8.93 (d, 1H, $J = 8$ Hz), 8.78 (d, 2H, $J = 7.8$ Hz), 8.65 (d, 1H, $J = 7.8$ Hz), 8.37 (m, 1H), 8.02 (m, 3H), 7.78 (m, 1H), 7.64 (d, 2H, $J = 5.4$ Hz), 7.42 (m, 3H), 7.06 (t, 1H).



The method used above on the preparation of $[Ru(trpy)(tfmbpy)(im)](PF_6)_2$ was followed in the synthesis of this compound.

The amounts used: $[Ru(Cl-trpy)(bpy)Cl]Cl$ (70 mg, 0.11 mmol) and $AgNO_3$ (56 mg, 0.33 mmol) were stirred in 11 mL water at 50°C for 24 hours. After filtering off the $AgCl$ and adding imidazole (37 mg, 0.55 mmol) the reaction was heated to reflux and stirred for 2 days. The product was an orange powder. Yield: 87 mg (quantitative yield). 1H -NMR (d_6 -DMSO), δ : 9.07 (s, 2H), 8.94 (d, 1H, J = 7.8 Hz), 8.80 (d, 2H, J = 8.4 Hz), 8.69 (d, 1H, J = 8.4 Hz), 8.46 (m, 1H), 8.36 (m, 1H), 8.12 (t, 2H, J = 8 Hz), 7.91 (m, 2H), 7.81 (d, 2H, J = 5.7 Hz), 7.49 (m, 3H), 7.14 (m, 2H), 6.9 (s, 1H), 5.99 (s, 1H).

Protein Protocols

Site-Directed Mutagenesis

All mutagenesis experiments were performed using the QuikChange mutagenesis kit (Stratagene). The appropriate primers were ordered from Invitrogen. The template DNA, W48F/Y72F/H83Q/Y108F-azurin, was obtained from Brian Leigh. Sequences were checked by DNA sequencing. Yuling Sheng executed site-directed mutagenesis for most of the mutants obtained.

Expression of Mutant Proteins

Following previously established protocol,^{24,38} the plasmids of the generated mutants were transformed into BL21 (DE3) Single Competent Cells (Novagen) and the bacteria were plated on LB-plates containing the antibiotic ampicillin. Colonies were

selected and inoculated in a 3 mL starter TB culture, supplemented with ampicillin (60 mg/mL). They were shaken for 7–8 hours at 37°C and the result was a cloudy beige solution. This solution was used to inoculate 6 x 1L TB media (70 mg/mL ampicillin) and the flasks were shaken for 20 hours at 37°C.

Cells were isolated by centrifuging the resulting mixture for 10 minutes at 5000 rpm. The cells were resuspended in sucrose solution and centrifuged for 10 min at 5000 rpm. The cells were then resuspended in cold MgSO₄ buffer solution and the mixture was allowed to stand for 10 minutes at 4°C, allowing for the bloated cells to lyse. The mixture was then centrifuged for 30 minutes at 10,000 rpm to isolate the lysed cell remains. The yellow supernatant was collected and 1 mL of the protease inhibitor PMF solution/100 mL supernatant was added. The solution was added to enough 1M NaOAc pH = 4.5 solution so that the final concentration of the NaOAc was 0.025 M. CuSO₄·5H₂O was added to the solution (0.25 g/50 mL). This mixture was allowed to stand for another week and stored at 4°C, allowing for precipitation of any undesirable protein and any other debris. (Azurin does not precipitate at this pH.) The mixture was then centrifuged at 5,000 rpm at 4°C for 10 minutes and the protein mixture was decanted and concentrated. The blue protein was purified by cation-exchange chromatography (see below) and stored in 25 mM NaOAc at 4°C until use. To check concentration of the protein, $\epsilon(628 \text{ nm}) = 5900 \text{ M}^{-1}\text{cm}^{-1}$.

Nitration of Tyrosine

Into a 25 mL round-bottom flask, 8.5 mL of a 70 μM solution of azurin in 25 mM NaP_i, pH 8 (though KP_i, pH 7.4 and 7.8 also work), was added. A concentrated stock

solution of azurin of known concentration was usually kept on hand, and was diluted to make this solution each time. The solution was stirred under argon for fifteen minutes, after which 1.5 mL of 1% v/v tetranitromethane/absolute ethanol was added dropwise via syringe in the dark. The reaction was stirred in the dark for 3 hours, after which it was opened up to air and run down a PD-10 desalting column to separate the protein from the tetranitromethane. Conversion can be checked for by exchanging the protein into pH 7.8 buffer and taking a UV-VIS spectrum. The protein was then purified using anion-exchange chromatography prior to being labeled.

Labeling Protein

To label the protein with $[\text{Ru}(\text{trpy})(\text{tfmbpy})]^{2+}$, the protocol developed by Dr. Angel Di Bilio was followed with minor modification.

$[\text{Ru}(\text{trpy})(\text{tfmbpy})\text{Cl}]\text{Cl}$ (10 mg, 0.014 mmol) and AgNO_3 (5 mg, 0.028 mmol) were added to a 2 dram vial equipped with a stir bar. The mixture was stirred in 1.4 mL water at 70°C for 24 hours. The resulting precipitate was filtered off, yielding a red-orange solution. To this solution, sodium phosphate was added until the pH of the solution was 7.2–7.8. If label precipitated, more water was added. This solution was utilized for the labeling.

Azurin was concentrated as much as it could be, resulting in a solution of 1–5 mM azurin. This solution was distributed among 1.7 mL Eppendorf tubes, 200 μL added to each. 1.3 mL label solution was added to each tube. The tubes were placed in a 37°C heating block and kept in the dark for 10 days.

The protein was isolated from excess label using Amicon Ultra-15 10,000 MWCO tubes (Millipore). Due to the high excess of ruthenium, the sample had to be washed extensively. Removal of the label is important; while the remaining label will be separated from protein on the chelating column (and it is straightforward to remove from the column), it is still preferable to load as little ruthenium onto the column as possible. After washing, the sample was purified by chelating column and cation-exchange chromatography, and, if the sample was a nitrotyrosine mutant, anion-exchange chromatography. The resulting protein is dark olive green in color. Purity was confirmed by mass spectrometry.

To label the protein with rhenium, a protocol outlined by Dr. Jeremiah Miller was used.¹³ The only changes made to the protocol were in the workup; PD-10 columns were found to be not necessary. Upon removal from the heating block, the protein was concentrated using Amicon Ultra-15 10,000 MWCO tubes and exchanged into 25 mM NaOAc, pH 4.52. The sample was allowed to stand at 4°C in the dark for 4 days to precipitate remaining rhenium. The sample was removed from the precipitate and washed further. Removal of excess rhenium is crucial in this case; rhenium is extremely difficult to remove from the chelating column. The sample was then purified using the chelating column, cation-exchange chromatography, and, in the cases utilizing nitrotyrosine, anion-exchange chromatography. The resulting protein is blue in color. The purity of the sample was checked with mass spectrometry.

Purification of Azurin

It cannot be emphasized enough that, to obtain pure samples of protein, clean FPLC columns must be used. Columns were always cleaned after the purification of each mutant, and cleaning procedures are detailed below. Column manuals should also be consulted for pepsin protocol when rigorous cleaning is desired (i.e., in times of frequent use, once every three months, in times of low use, once every six months/every time purification is started up again).

Chelating Column

The chelating column used was 5 mL HiTrap chelating column (GE Healthcare).

Solutions used for HiTrap are listed below in **Table 2.5**.

| Buffer | Composition |
|---------------|--|
| Buffer A | 20 mM NaP _i , 750 mM NaCl, pH 7.2 |
| Buffer B | 20 mM NaP _i , 750 mM NH ₄ Cl, pH 7.2 |
| Cu solution | 100 mM CuSO ₄ |
| EDTA solution | 25 mM NaEDTA, pH 8.8 |

Table 2.5. Solutions for HiTrap Chelating Column.

A flow rate of 2 to 4 mL/min was utilized in this protocol.

In preparation for protein purification, the column was equilibrated to Buffer A by running 15 mL of the buffer through the column. After equilibration, 2 mL Cu solution was loaded onto the column and the column was allowed to equilibrate. If not enough copper was added, another 1 mL of the Cu solution was loaded. After copper was loaded on the column, 15 mL Buffer B was run through to remove excess copper. 30 mL of Buffer A was run through afterwards to equilibrate the column for protein purification.

The sample loaded onto the column for purification was 200–500 μM , and can always be less; it is not recommended to be much more concentrated, as overloading the column will result in no separation at all. Usually, 1.5 mL of the protein solution was loaded onto the column each run. The sample was loaded onto the column using buffer A.

Separation by chelating column is straightforward; the exposed histidine of the unlabeled protein will bind to the copper of the column and become immobilized. The labeled protein, where the label blocks access to the histidine, will not be deterred and simply pass through the column. The method utilized is summarized below in **Table 2.6**.

| mLs into run | % Buffer B |
|--------------|------------|
| 0 | 0 |
| 25 | 0 |
| 27 | 100 |
| 60 | 100 |
| 62 | 0 |
| 75 | 0 |

Table 2.6. Method utilized to purify labeled proteins on the chelating column

The copper was stripped off the column after use, or between mutants. To remove the copper, 2 mL EDTA solution was loaded onto the column and the column was allowed to equilibrate. If any copper remained on the column (evident from lingering color on the column), EDTA loading and equilibration was repeated until the copper was removed.

If copper precipitated on the column, removal was achieved by preparing a 10 mL superloop with 10 mL EDTA solution. The solution was slowly loaded onto the column, at a rate of 0.01 or 0.1 mL/min, and was left thus for approximately 8–10 hours.

If rhenium precipitated on the column, a methanol gradient was run, often more than once, to remove the metal. In this method, the flow rate was ~1 mL/min. The column should not remain under 100% methanol for too long.

| mLs into run | % Buffer B |
|--------------|------------|
| 0 | 0 |
| 50 | 100 |
| 100 | 0 |
| 130 | 0 |

Table 2.7. Methanol gradient method run to remove metal labels from chelating columns and ion-exchange columns. Buffer A is milli Q water, buffer B is HPLC grade methanol.

After use, the column was stored in 20% absolute ethanol/milli Q water.

Cation-Exchange Chromatography

Cation-exchange chromatography was accomplished using a Mono S HR 10/10 column (GE Healthcare). It was executed on proteins after metallation and prior to labeling, proteins after labeling (subsequent to the chelating column), and prior to laser experiments. Solutions used for Mono S are listed below in **Table 2.8**.

| Buffer | Composition |
|------------------|-----------------------|
| Buffer A | 25 mM NaOAc, pH 4.52 |
| Buffer B | 300 mM NaOAc, pH 4.52 |
| EDTA solution | 25 mM NaEDTA, pH 8.8 |
| Acetate solution | 2 M NaOAc |
| Base solution | 2 M NaOH |
| Salt solution | 2 M NaCl |

Table 2.8. Solutions for Mono S column

The MonoS column used in these studies was a bit old, so the flow rate had to be kept to 1 to 2 mL/min.

In preparation for purification, 30 mL Buffer B was run through the column, then 50 mL Buffer A. The sample loaded onto the column for purification was 200–500 μM , and can always be less; it is not recommended to be much more concentrated, as overloading the column will result in no separation at all. Usually, 1.5 mL of the protein solution was loaded onto the column each run. The sample was loaded onto the column using buffer A.

The active component of the resin of the Mono S column is $-\text{CH}_2-\text{SO}_3^-$. Proteins are separated by their cationic charge. Apo azurin usually goes straight through the column. Zinc and copper-substituted azurins usually elute at around 20% Buffer B. The gradient must be proceeded through slowly to achieve separation (**Table 2.9**). For optimal purification, the gradient was held when the blue band of protein started moving on the column, and was continued only when the last of the protein had come off the column.

| mLs into run | % Buffer B |
|--------------|------------|
| 0 | 0 |
| 25 | 0 |
| 125 | 100 |
| 145 | 100 |
| 147 | 0 |
| 180 | 0 |

Table 2.9. Method utilized to purify azurin on the Mono S column

Every few runs, even if the runs were being done on the same mutant, the column was subjected to a quick cleaning: the column was turned upside down, and equilibrated to milli Q water. The following sequence was then executed: 2 mL load salt solution,

equilibration, 2 mL load acetate solution, equilibration, 2 mL load salt solution, equilibration, 2 mL load base solution, equilibration, 2 mL load salt solution, equilibration. If a different mutant was going to be purified on the column, this cleaning sequence was repeated a few more times.

If orange or yellow residue remained on the column, metal label was contaminating the column. The column was turned upside down and the methanol gradient (delineated above in **Table 2.7**) was executed.

If zinc azurin was being purified, the Mono S column was subjected to at least five 2-mL loads of the EDTA solution to remove any copper on the column, so that copper contamination can be avoided.

When not in use, the column was stored in 20% absolute ethanol/milli Q water.

Anion-Exchange Chromatography

Anion-exchange chromatography was accomplished using a Mono Q HR 10/10 column (GE Healthcare). It was executed on proteins with nitrotyrosine after the nitration reaction and after labeling (subsequent to the chelating column), and prior to laser experiments. Solutions used for Mono Q are listed below in **Table 2.10**.

| Buffer | Composition |
|------------------|-----------------------------|
| Buffer A | 50 mM DEA, pH 8.8 |
| Buffer B | 50 mM DEA, 1 M NaCl, pH 8.8 |
| Acetate solution | 2 M NaOAc |
| Base solution | 2 M NaOH |
| Salt solution | 2 M NaCl |

Table 2.10. Solutions used for Mono Q

In preparation for purification, 30 mL Buffer B was run through the column, then 50 mL Buffer A. The sample loaded onto the column for purification was 200–500 μM , and can always be less; it is not recommended to be much more concentrated, as overloading the column will result in no separation at all. Usually, 1.5 mL of the protein solution was loaded onto the column each run. The sample was loaded onto the column using buffer A.

The active component of the resin of the Mono Q column is $-\text{CH}_2\text{-N}(\text{CH}_3)_3^+$. Proteins are separated by their anionic charge. Because the column is being carried out at high pH, if the tyrosine has been nitrated, it should be in the deprotonated form and should be separated on the column from non-nitrated azurin. The non-nitrated azurin usually elutes early, often not even needing Buffer B for elution. Nitrated azurin elutes at around 50% Buffer B. The gradient must be proceeded through slowly to achieve separation (**Table 2.11**). For optimal purification, the gradient was held when the blue-green band of protein started moving on the column, and was continued only when the last of the protein had come off the column.

| mLs into run | % Buffer B |
|--------------|------------|
| 0 | 0 |
| 25 | 0 |
| 125 | 100 |
| 145 | 100 |
| 147 | 0 |
| 180 | 0 |

Table 2.11. Method utilized to purify azurin on the Mono Q column

Every few runs, even if the runs were being done on the same mutant, the column was subjected to a quick cleaning: the column was turned upside down, and equilibrated to milli Q water. The following sequence was then executed: 2 mL load salt solution,

equilibration, 2 mL load acetate solution, equilibration, 2 mL load salt solution, equilibration, 2 mL load base solution, equilibration, 2 mL load salt solution, equilibration. If a different mutant was going to be purified on the column, this cleaning sequence was repeated a few more times.

If orange or yellow residue remained on the column, metal label was contaminating the column. The column was turned upside down and the methanol gradient (delineated above in **Table 2.7**) was executed.

When the column was not in use, it was stored in 20% absolute ethanol/milli Q water.

Electrochemical Measurements

Measurements were made with the help of Brian S. Leigh. Measurements were made on a Model 660 Electrochemical Workstation (CH-Instrument, Austin, TX) in a two-compartment cell with a glassy carbon working electrode, a platinum wire counter electrode, and a silver/silver nitrate reference electrode. 100 mM tetrabutylammonium tetrafluoroborate was prepared in dry degassed acetonitrile as electrolyte. Measurements were carried out at room temperature.

Circular Dichroism Measurements

CD spectra were taken on an Aviv 62ADS spectropolarimeter (Aviv Associates, Lakewood, NJ). Measurements were carried out in a 1 mm cuvette at room temperature. Accompanying UV-VIS measurements were also measured with the 1 mm cuvette. Data was recorded between 190 nm and 260 nm with a band-pass of 1.5 nm.

Laser Spectroscopy & Analysis

Time-resolved emission and absorbance measurements were made on custom-made laser setup Nanosecond-I in the Beckman Institute Laser Resource Center. The laser setup has already been thoroughly outlined and explained elsewhere,²⁴ so only basic details are summarized here. A frequency-tripled Nd:YAG laser from Spectra-Physics emits 355 nm pulses, 10 ns in duration. Measurements carried out on rhenium systems were excited by this laser. Measurements carried out on the ruthenium systems were excited by laser light from a Spectra-Physics MOPO, which was pumped by the Nd:YAG. The laser power was adjusted using a quarter-wave plate so that the laser light exciting the sample had a power of 1 mJ/pulse. For the most part, transient absorption was probed for with white light from a xenon arc lamp, which was run in a continuous mode, or set to generate 500 μ s pulses of brighter light. Transient absorption measurements at 632.8 nm were made using a HeNe laser probe to limit the collection of emission from the label at that wavelength.

Sample Preparation

25 to 50 μ M samples of protein in freshly made 25 mM KP_i buffer, in the pH range 7.0 to 7.8, were added to 1 cm path length cuvettes and degassed by fifteen quick pump purges, stirring under argon for fifteen minutes, and another quick fifteen pump purges. Generation of bubbles in the sample during the degassing was unavoidable, but was kept to a minimum by careful watching of the sample.

To reduce the copper center for certain measurements, sodium dithionite was added until the blue color of the sample disappeared. This sample was washed with

buffer to remove excess dithionite; if the blue reappeared, more dithionite would be added and washing would be repeated. The sample was then added to the cuvette and degassed as described above.

To reduce the copper center in samples with nitrotyrosine residues, dithionite could not be used; the dithionite reduced the nitrotyrosine to aminotyrosine. Instead, the green sample was placed in the cuvette with a stir bar and a small scrap of Pt mesh (1 mm by 3 mm) and the solution was deaerated and put under hydrogen gas for 15 minutes, deaerated and put under hydrogen gas for another 4 to 8 hours (the reaction time depended on which mutant was being reduced). It is important that the stir bar agitates the scrap of Pt. Because the H₂/Pt reduction, as well as reducing the copper, also reduces any oxygen present into water, no further degassing was necessary, though the sample was usually put under argon for laser experiments.

Data Analysis

The data obtained from the Nanosecond-I laser setup was analyzed using Igor Pro 5.01 (WaveMetrics, Inc., Lake Oswego, OR). Data was fit with a non-linear least-square algorithm to function with single (n=1), double (n=2), or triple (n=3) exponential decays (**Equation 2.1**). The reported τ values are calculated from the k_n obtained from the fit (**Equation 2.2**).

$$I(t) = c_0 + \sum_n c_n e^{-k_n t} \quad \text{Eq. 2.1}$$

$$\tau_n = \frac{1}{k_n} \quad \text{Eq. 2.2}$$

2.6 REFERENCES

- (1) Sutherland, I. W.; Wilkinson, J. F. *J. Gen. Microbiol.* **1963**, *30*, 105–112.
- (2) Antonini, E.; Finazzi-Agro, A.; Avigliano, L.; Guerrieri, P.; Rotilio, G.; Mondovi, B. *J. Biol. Chem.* **1970**, *245*, 4847–4849.
- (3) Solomon, E. I.; Hare, J. W.; Dooley, D. M.; Dawson, J. H.; Stephens, P. J.; Gray, H. B. *J. Am. Chem. Soc.* **1980**, *102*, 168–178.
- (4) Adman, E. T. *Adv. Protein Chem.* **1991**, *42*, 145–197.
- (5) Gray, H. B.; Malmstrom, B. G.; Williams, R. J. P. *J. Biol. Inorg. Chem* **2000**, *5*, 551–559.
- (6) Solomon, E. I.; Randall, D. W.; Glaser, T. *Coordin. Chem. Rev.* **2000**, *200-202*, 595–632.
- (7) Pascher, T.; Karlsson, B. G.; Nordling, M.; Malmstrom, B. G.; Vanngard, T. *Eur. J. Biochem.* **1993**, *212*, 289–296.
- (8) Chang, T. K.; Iverson, S. A.; Rodrigues, C. G.; Kiser, C. N.; Lew, A. Y. C.; Germanas, J. P.; Richards, J. H. *P. Natl. Acad. Sci. USA* **1991**, *88*, 1325–1329.
- (9) Langen, R.; Chang, I. J.; Germanas, J. P.; Richards, J. H.; Winkler, J. R.; Gray, H. B. *Science* **1995**, *268*, 1733–1735.
- (10) Langen, R.; Colon, J. L.; Casimiro, D. R.; Karpishin, T. B.; Winkler, J. R.; Gray, H. B. *J. Biol. Inorg. Chem* **1996**, *1*, 221–225.
- (11) Crane, B. R.; Di Bilio, A. J.; Winkler, J. R.; Gray, H. B. *J. Am. Chem. Soc.* **2001**, *123*, 11623–11631.
- (12) Wehbi, W. A., California Institute of Technology, 2003.
- (13) Miller, J. E., California Institute of Technology, 2003.
- (14) Harriman, A. *J. Phys. Chem.* **1987**, *91*, 6102–6104.
- (15) Magnuson, A.; Frapart, Y.; Abrahamsson, M.; Horner, O.; Akermark, B.; Sun, L.; Girerd, J. J.; Hammarstrom, L.; Styring, S. *J. Am. Chem. Soc.* **1999**, *121*, 89–96.
- (16) Sjodin, M.; Styring, S.; Akermark, B.; Sun, L.; Hammarstrom, L. *J. Am. Chem. Soc.* **2000**, *122*, 3932–3936.
- (17) Remers, W. A. In *Indoles, Part One*; Houlihan, W. J., Ed.; Wiley-Interscience: New York City, 1972; Vol. 25, 1–226.
- (18) Leigh, B.S. (*unpublished work*).
- (19) Riordan, J. F.; Sokolovsky, M.; Vallee, B. L. *J. Am. Chem. Soc.* **1966**, *88*, 4104–4105.
- (20) Sokolovsky, M.; Riordan, J. F.; Vallee, B. L. *Biochemistry* **1966**, *5*, 3582–3589.
- (21) Riordan, J. F.; Sokolovsky, M.; Vallee, B. L. *Biochemistry* **1967**, *6*, 358–361.
- (22) Bruice, T. C.; Gregory, M. J.; Walters, S. L. *J. Am. Chem. Soc.* **1968**, *90*, 1612–1619.
- (23) Riordan, J. F.; Vallee, B. L.; Hirs, C. H. W.; Serge, N. T. In *Methods in Enzymology*; Academic Press: 1972; Vol. 25, 515–521.
- (24) Miller, J.; Di Bilio, A.; Wehbi, W.A.; Green, M.T.; Museth, A.K.; Richards, J.H.; Winkler, J.R.; Gray, H.B. *BBA Bioenergetics* **2004**, *1655*, 59–63.
- (25) Winkler, J. R.; Gray, H. B. *Chem. Rev.* **1992**, *92*, 369–379.

- (26) Mines, G. A.; Bjerrum, M. J.; Hill, M. G.; Casimiro, D. R.; Chang, I. J.; Winkler, J. R.; Gray, H. B. *J. Am. Chem. Soc.* **1996**, *118*, 1961–1965.
- (27) Di Bilio, A. J.; Hill, M. G.; Bonander, N.; Karlsson, B. G.; Villahermosa, R. M.; Malmstrom, B. G.; Winkler, J. R.; Gray, H. B. *J. Am. Chem. Soc.* **1997**, *119*, 9921–9922.
- (28) Di Bilio, A. J.; Dennison, C.; Gray, H. B.; Ramirez, B. E.; Sykes, A. G.; Winkler, J. R. *J. Am. Chem. Soc.* **1998**, *120*, 7551–7556.
- (29) Sokolovsky, M.; Harell, D.; Riordan, J. F. *Biochemistry* **1969**, *8*, 4740–4745.
- (30) Johnson, E. C.; Sullivan, B. P.; Salmon, D. J.; Adeyemi, S. A.; Meyer, T. *J. Inorg. Chem.* **1978**, *17*, 2211–2215.
- (31) Durham, B.; Pan, L. P.; Long, J. E.; Millett, F. *Biochemistry* **1989**, *28*, 8659–8665.
- (32) Durham, B.; Pan, L. P.; Hahm, S.; Long, J.; Millett, F. *Adv. Chem. Ser.* **1990**, 181–193.
- (33) Arjara, G. (*unpublished results*).
- (34) Sullivan, B. P.; Calvert, J. M.; Meyer, T. *J. Inorg. Chem.* **1980**, *19*, 1404–1407.
- (35) Takeuchi, K. J.; Thompson, M. S.; Pipes, D. W.; Meyer, T. *J. Inorg. Chem.* **1984**, *23*, 1845–1851.
- (36) Chan, K. S.; Tse, A. K. S. *Synthetic Commun.* **1993**, *23*, 1929–1934.
- (37) Sullivan, B. P.; Salmon, D. J.; Meyer, T. *J. Inorg. Chem.* **1978**, *17*, 3334–3341.
- (38) Sheng, Y. (*unpublished results*).